TAMPEREEN TEKNILLINEN YLIOPISTO
TAMPERE UNIVERSITY OF TECHNOLOGY

MIKA HELMINEN

OPTIMIZATION OF A TRUSSED STEEL PORTAL FRAME

Master of Science thesis

Examiner: Dr. Kristo Mela
Examiner and topic approved by the
Faculty Council of the Faculty of
Business and Built Environment
on 25th September 2017

ABSTRACT

MIKA HELMINEN: Optimization of a trussed steel portal frame
Tampere University of Technology
Master of Science thesis, 63 pages, 2 Appendix pages
December 2017
Master's Degree Programme in Civil Engineering
Major: Structural Engineering
Examiner: Dr. Kristo Mela
Keywords: Optimization, mass minimization, cost minimization, steel structures, portal frame

The goal of this study was to develop a sizing optimization method for a trussed steel portal frame that meets strength and stability criteria presented in Eurocode 3. In addition to strength and stability of the frame members, the strength and geometrical restrictions of welded truss joints were also taken into account. The method was required to find a feasible solution of good quality within appropriate calculation time. Optimization and the finite element model of the frame were both implemented in MATLAB.

A four-stage optimization procedure was developed. This procedure includes two subproblems which are both solved first with continuous variables and then with discrete variables. The cross-sectional dimensions of square hollow section profiles were treated as design variables of the optimization problem. An interior-point algorithm was used to solve the continuous problem. The discrete problem was solved by Genetic Algorithm.

The method was tested with different structural setups in which the loading conditions and the geometry of the frame were changed. Both minimum-mass and minimum-cost solutions were searched. The distribution of total mass and cost was studied by the structural components. Additionally, the conflict of mass and cost was studied. High-strength steels were also considered in the study. Based on the results of optimization it was concluded that the four-stage procedure seems to be well-suited for the optimization problem of a trussed steel portal frame.

TIIVISTELMÄ

MIKA HELMINEN: Teräksisen ristikkorakenteisen portaalikehän optimointi
Tampereen teknillinen yliopisto
Diplomityö, 63 sivua, 2 liitesivua
Joulukuu 2017
Rakennustekniikan koulutusohjelma
Pääaine: Rakennesuunnittelu
Tarkastajat: TkT Kristo Mela
Avainsanat: Optimointi, massan minimointi, kustannusten minimointi, teräsrakenteet, portaalikehä

Tämän työn tavoitteena oli kehittää mitoitusoptimointimenetelmä teräksiselle ristikkorakenteiselle portaalikehälle, joka täyttää Eurokoodi 3:n esittämät vaatimukset lujuudelle ja stabiilisuudelle. Sauvojen lujuuden ja stabiilisuuden lisäksi rajoitusehdoissa huomioitiin myös ristikon hitsattujen liitosten kestävyydet ja geometriaehdot. Menetelmältä vaadittiin hyvälaatuisen käyvän ratkaisun löytämistä kohtuullisen laskenta-ajan kuluessa. Optimointi ja kehän elementtimallin rakentaminen tehtiin MATLAB-ohjelman avulla.

Optimointimenetelmäksi kehitettiin nelivaiheinen menettely. Tämä menettely sisältää kaksi alitehtävää, jotka molemmat ratkaistaan ensin jatkuvilla muuttujilla ja tämän jälkeen diskreeteillä muuttujilla. Optimointitehtävän suunnittelumuuttujina käsiteltiin neliöputkiprofiilin poikkileikkausmittoja. Interior-point algoritmia käytettiin jatkuvan tehtävän ratkaisemiseen. Diskreetti tehtävä ratkaistiin puolestaan Geneettisellä Algoritmilla.

Menetelmää testattiin erilaisilla rakenteilla, joissa vaihdeltiin kuormitusta ja kehän geometriaa. Optimoinnissa haettiin sekä massa- että kustannusoptimeja. Kehän kokonaismassan ja kustannusten jakautumista tutkittiin rakenneosittain. Lisäksi massa- ja kustannusoptimeja vertailtiin keskenään. Myös korkealujuusterästä sisältävää kehää tutkittiin. Testitapausten tulosten perusteella todettiin, että nelivaiheinen menettely näyttää sopivan hyvin teräksisen ristikkorakenteisen portaalikehän optimointitehtävään.

PREFACE

This thesis was done for SSAB Europe Oy. The work was done in facilities of the Research Center of Metal Structures in Tampere University of Technology. The project started in February 2017 and continued until November 2017. This whole process has been heavy but rewarding and it has given me a good picture of the various phases of the research project.

I would like to thank SSAB for the opportunity of doing my master of science thesis on a very interesting and challenging subject. Special thanks belong to the supervisor and examiner of my thesis, Dr. Kristo Mela whose enthusiasm towards structural optimization is inspiring. His guidance and the MATLAB codes that he had wrote helped greatly in getting started with my thesis. I would also like to thank my colleagues in the Research Center of Metal Structures for the discussions on my thesis and advices on the use of LaTeX and MATLAB.

My studentship in Tampere University of Technology has been memorable. I've got a lot of friends with whom I have spent leisure time and done schoolworks. Thanks to them the time at the university was unforgettable. I also thank my family who has always supported and believed in me. Lastly, I would like to thank my girlfriend Laura who has brought joy and happiness into my life.

Tampere, 17.11.2017

Mika Helminen

CONTENTS

LIST OF FIGURES

LIST OF TABLES

LIST OF ABBREVIATIONS AND SYMBOLS

Abbreviations

FEM	Finite element method
GA	Genetic Algorithm
HSS	High-strength steel
NAND	Nested analysis and design
SAND	Simultaneous analysis and design
SHS	Square hollow section

Latin symbols

a	The weld size
A	Cross-section area
A_0	Cross-section area of a chord
$A_{0,est}$	Estimated cross-section area of a chord
A_h	Sawing area of horizontal parts of the profile
A_p	Painting area
A_t	Cross-section area of the sawed end
A_u	Circumference of the cross-section
A_v	Shear area
a_w	Coefficient for reducing bending capacity
b	Cross-section width
b_{eff}	Effective width for a brace member
$b_{\mathrm{e,p}}$	Effective width for punching shear
c	Dimension for cross-section classification
C	Total cost of the frame
C_B	Blasting cost
c_{CP}	Cost of painting consumables
c_{CPA}	Cost of welding consumables
c_{CS}	Cost of sawing consumables
c_{EnPA}	Energy cost of welding
c_{EnS}	Energy cost of sawing
c_{EqPA}	Welding equipment cost
c_{LP}	Unit labour cost of painting
c_{LPA}	Unit labour cost of welding

C_M	Material cost
C_{my}	Equivalent uniform moment factor
C_P	Painting cost
C_{PA}	Welding cost
c_{REP}	Real estate investment cost of painting
c_{REPA}	Real estate investment cost of welding
c_S	Constant for sawing costs
C_S	Sawing cost
c_{SeP}	Real estate maintenance cost of painting
c_{SePA}	Real estate maintenance cost of welding
c_{SM}	Unit cost of the profile
e	Joint eccentricity
E	Elastic modulus
E_d	Design value of forces
f	Objective function
$\mathbf{F}$	Global load vector
F_s	Parameter
F_{sp}	Parameter
f_y	Yield strength
$f_{\mathrm{y}0}$	Yield strength of a chord
g	Joint gap
g_i, g_j	Constraints
h	Cross-section height
h_0	Cross-section height of a chord
H_1, H_2, H_3	Dimensions of the frame
h_b	Cross-section height of a brace member
h_{bc}	Cross-section height of a bottom chord
h_c	Cross-section height of a column
h_s	Sawing height
h_{tc}	Cross-section height of a top chord
i	Radius of inertia
$\mathbf{K}$	Global stiffness matrix
k_n	Parameter
k_{yy}, k_{zy}	Interaction factors
l	Length of the frame member
L	Span of the truss
L_{cr}, $L_{cr,y}$, $L_{cr,z}$	Buckling length
L_{fw}	The weld length
M_{beam}	Bending moment of a single-span beam

$M_{col,h}$	Bending moment of a column from horizontal loads
$M_{col,v}$	Bending moment of a column from vertical loads
$M_{\mathrm{c,Rd}}$	Design bending resistance
M_{Ed}	Design bending moment
$M_{\mathrm{N,Rd}}$	Reduced design bending resistance
$M_{\mathrm{pl,Rd}}$	Plastic design bending resistance
M_{Rk}	Characteristic bending resistance
n	Parameter
n_B	Number of braces
N_{beam}	Normal force of a beam
$N_{\mathrm{b,Rd}}$	Design buckling resistance
$N_{\mathrm{c,Ed}}$	Design compression force
n_{E}	Number of the frame members
N_{Ed}	Design axial force
$N_{\mathrm{Ed,i}}$	Design axial force acting on brace i
$n_{\mathrm{E,t}}$	Number of the truss members
n_J	Number of joints
$N_{\mathrm{pl,Rd}}$	Plastic design axial resistance
n_{pop}	Population size in GA
$N_{\mathrm{Rd,i}}$	Design joint resistance for brace i
N_{Rk}	Characteristic axial resistance
n_{sym}	Number of symmetry pairs of braces
$N_{\mathrm{t,Ed}}$	Design tension force
n_{var}	Number of variables
p_1	Top chord load
p_2	Bottom chord load
p_{SB}	Price of the saw blade
Q	Efficiency
q_1, q_2	Wind loads
r	Bending radius of a cross-section
R_d	Design value of resistance
S	Feeding speed
S_m	Parameter
S_t	The durability of the blade
t	Wall thickness of a cross-section
t_0	Wall thickness of a chord
t_b	Wall thickness of a brace member
t_{bc}	Wall thickness of a bottom chord
t_c	Wall thickness of a column

t_{mv}	Sawing thickness of the vertical part
T_{NS}	Non-productive sawing time
T_{PP}	Productive painting time
T_{PPA}	Productive welding time
T_{PS}	Productive sawing time
T_{PTa}	Tacking time
T_{Pw}	Welding time
t_{tc}	Wall thickness of a top chord
$\mathbf{u}$	Nodal displacement vector
u_S, u_P, u_{PA}	Utilization rates of cost functions
V_{beam}	Shear force of a single-span beam
V_{Ed}	Design shear force
$V_{\mathrm{pl,Rd}}$	Plastic design shear resistance
W	Total mass of the frame
W_{el}	Elastic section modulus
W_{pl}	Plastic section modulus
$\mathbf{x}$	Variable vector

Greek symbols

α	Imperfection factor
β	Parameter
γ	Parameter
γ_{M0}, γ_{M1}, γ_{M5}	Partial safety factors
ϵ	Parameter for cross-section classification
η	Parameter
θ_1, θ_2	Joint angles
$\bar{\lambda}$	Non-dimensional slenderness
ρ	Density of steel
Φ	Value to determine the reduction factor for buckling
χ, χ_y, χ_z	Reduction factor for buckling
χ_{LT}	Reduction factor for lateral-torsional buckling

1. INTRODUCTION

1.1 Background

Framed structures made of steel profiles are often used as load-bearing structures in many different halls and industrial buildings. There is wide range of different kind of prefabricated steel profiles such as I-sections or structural hollow sections. Especially structural hollow sections are popular in frames and lattice structures. A few examples of tubular frames are shown in Fig. 1.1. Reasons for their popularity are e.g. high torsional and bending stiffness. Also high buckling resistance of hollow sections makes them usable in long spans. Despite their high stiffness and capacity hollow sections are very light. Tubular structures have also been studied extensively and many design standards and guides have been written [11, 12, 26, 27]. Another advantage of hollow sections is a wide selection of different size profiles.

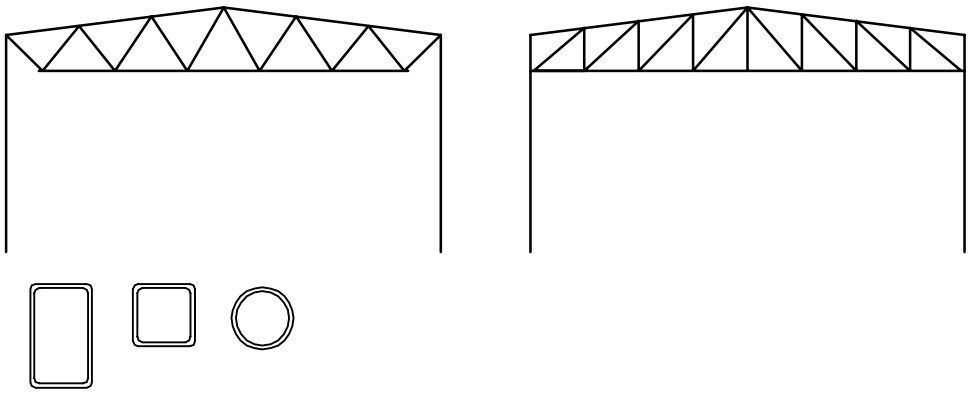

Figure 1.1: *Tubular frames and hollow section profiles. Rectangular (RHS), square (SHS) and circular hollow section (CHS).*

In practical design work, designers choose few different structures at the beginning of the project on the basis of their own experience and intuition. These options are compared to each other and the most suitable option is chosen. Optimization offers an alternative approach to this conventional design process. The purpose of optimization is to find either minimum or maximum value of the objective function such as weight or cost of the structure.

The biggest advantage of optimization is that it can evaluate much more different options than the conventional design approach. The beginning of optimization process requires a lot of time and care because design variables, objective function and constraints must be decided. Benefits of optimization will come up later in design process when larger number of structures can be evaluated with the help of improved computer calculation capacities. Especially in big and complex structures optimization shows its strength when the amount of evaluated options is huge. The basic concepts of structural optimization have been explained in [2, 19].

There are three ways to approach structural optimization problem: sizing, shape and topology. Sizing optimization aims to smallest possible profiles when geometry of the structure is decided in advance. In this case cross-sectional dimensions such as plate thickness and outer dimensions of cross-section are treated as design variables. In shape optimization the purpose is to find the most suitable shape for the structure e.g. the height of a roof truss. In topology optimization the goal is to discover the best way to place components in a structure. For instance, the number and position of brace members in a truss can be changed. These three different approaches are described in Fig. 1.2. Usually practical structural optimization problem includes all these approaches and the best solution can be obtained in this way.

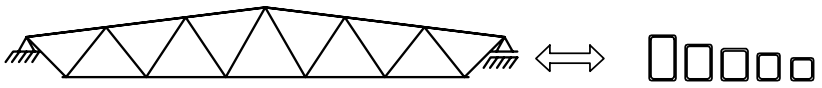

(a) Sizing optimization.

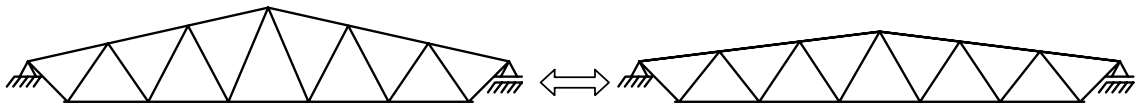

(b) Shape optimization.

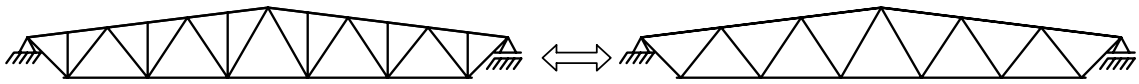

(c) Topology optimization.

Figure 1.2: *Sizing, shape and topology optimization.*

Formulation of optimization problem requires objective function, design variables and constraints. For manufacturer and designer the most interesting issue is usually cost. Often the goal of optimization is to minimize cost so that constraints keep manufacturing of structure possible and convenient and ensure strength of the structure. However, in steel structures the mass is often chosen as objective function instead of cost. The reason for this is that mass optimum can be presumed to be close to cost optimum. Mass functions are also simpler to form compared to cost functions

that contain more different parameters and coefficients. This makes mass functions easier to handle in optimization. In practice cost includes e.g. sawing, welding and painting in addition to the consumption of material. The minimization of cost in welded steel structures has been studied by [13, 23, 24].

The right choice of design variables is essential in optimization. The variables influence on difficulty of solving the problem. There are two types of variables: continuous and discrete. Continuous variable can get any value between lower and upper bound. Discrete variable can get value only from certain set of values. Discrete optimization problem is more difficult to solve than continuous problem. Sizing optimization is a good example of a problem where discrete variables are used. Manufacturers have a certain catalog of profiles so only those cross-sections can be allowed in optimization result. When a problem contains both types of variables the problem is called mixed-integer. Methods for handling discrete variables in structural optimization have been presented in articles of Arora [1], Arora & Huang [3], Arora, Huang & Hsieh [4] and Thanedar & Vanderplaats [30]. Textbooks on discrete and mixed-integer optimization have been written by Floudas [15] and Nemhauser & Wolsey [25].

Design code requirements must be acknowledged in constraints so that optimization results would be practical. This causes challenges because design criteria include lots of terms and functions which are piecewise-defined. This leads to nonlinear and nonconvex problem including discrete variables and awkward constraints. Solution methods that require derivation of objective and constraint function are therefore not suitable for the problem. This limits the number of suitable optimization methods.

One of the most popular solution methods for these kind of problems are heuristic algorithms which have been studied extensively. These algorithms try to mimic phenomena occurring in nature such as biological development of species or behavior of birds. *Genetic Algorithm* (GA) is probably the most common method among these algorithms. It can not guarantee global optimum solution but it can find a feasible and good solution within a reasonable time.

There are also many different ways to formulate the optimization problem. Arora and Wang [5] presented review of formulation methods for structural systems. The most common approach formulating the problem is called conventional formulation where only the design variables are selected as optimization variables. The response quantities such as displacements, stresses and internal forces are described as implicit functions of design variables. This approach is also called the *nested analysis and design* (NAND). Advantages of this approach are that there are least number of

variables and also intermediate solutions may be usable. Also equilibrium equation is satisfied at each iteration. On the other hand NAND formulation has also some disadvantages. Solving the equilibrium equation at each iteration can be expensive and evaluation of constraints requires analysis since constraints are implicit functions of the variables.

The other way to approach structural optimization problem is called *Simultaneous analysis and design* (SAND). This formulation includes some of the state variables e.g. displacements in optimization variables in addition to the common design variables. The equilibrium equation is then written as equality constraint in terms of the variables. The benefits of SAND formulation are for example that equilibrium equation is not solved at every iteration and some of the constraints may become linear. The strengths of this formulation come up best in topology optimization. Disadvantages are that number of variables and constraints increases and intermediate solutions may not be usable. [5]

Previously optimization of frame structures has been studied by Greiner, Winter & Emperador [16] who used Genetic Algorithm for minimum-mass problem. Guerlement et al. [17] studied optimization of a single portal frame by using only member strength constraints from Eurocode 3. Wang and Arora [32] compared difference between conventional formulation and SAND formulation in optimization of frames. Jalkanen [22] compared efficiency of different heuristic algorithms in tubular truss optimization.

1.2 The aim and scope of the study

The goal of this study is to devise a procedure for solving an optimization problem of a steel portal frame consisting of two columns and a roof truss. The main criterion for the method is reasonable calculation time. NAND formulation is applied in formulation of the optimization problem. Both minimum-mass and minimum-costs solutions are searched. Structural analysis is carried out in accordance with the design rules and criteria of Eurocode 3. Strength and stability of members are included in constraints as well as strength and geometry rules of truss joints. High-strength steels (HSS) are also taken into consideration.

Only SHS profiles from cross-section classes 1 and 2 are treated because they are most common profiles in tubular steel trusses. Also only sizing optimization is considered i.e. geometry of the frame and topology of the truss are decided and fixed before optimization.

The first Chapter gives an overview of theoretical background of this thesis and presents the goals and outline of the study. Chapter 2 presents the design aspects of the structural analysis and design code requirements for portal frames. Chapter 3 describes optimization method and algorithms used in this thesis. In Chapter 4, the optimization problem is formulated. Also design variables, constraints and objective functions are introduced. Chapter 5 introduces calculation examples and their results. Finally Chapter 6 summarizes the results and the most relevant observations.

2. DESIGN OF PORTAL FRAMES

This thesis focuses on a portal frame with two columns as vertical members and a roof truss as horizontal structure. The structure is shown in Fig. 2.1 All members of the frame are SHS profiles. Profiles are chosen from the SHS-catalog of SSAB presented in Appendix A. The catalog includes steel grades S355, S420 and S700. Structural analysis is done in accordance with the design rules based on Eurocode 3. Member strength and stability are checked. Also geometrical restrictions and resistances of welded truss joints are taken into account. Second-order effects are ignored so only first-order analysis is used.

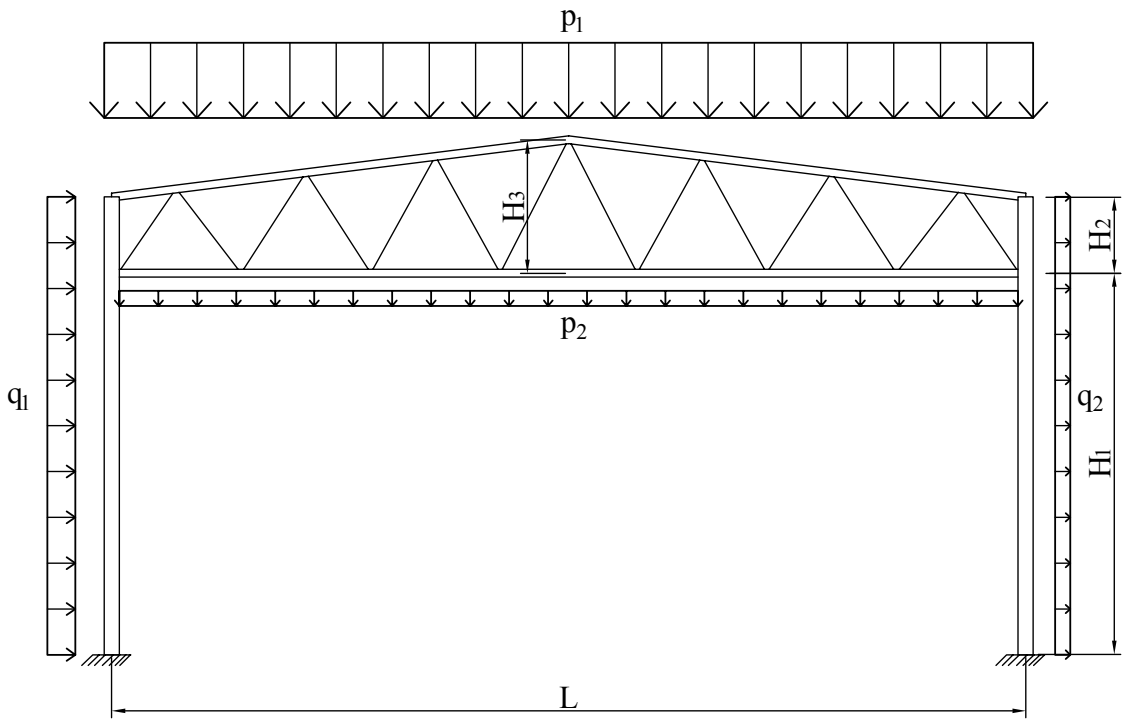

Figure 2.1: *Trussed steel portal frame.*

EN 1991-1-1 [10] determines the loads used for structural calculations. The loads acting on the frame are snow load, dead loads and wind load. Dead loads include roof structures, hanging load on the bottom chord and structural self-weight of the frame.

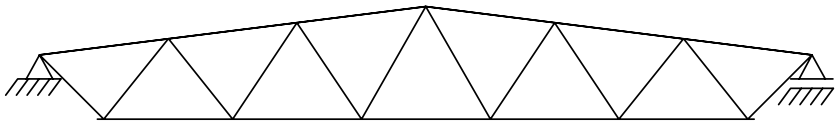

(a) K-truss.

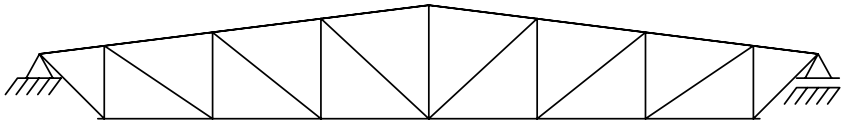

(b) N-truss.

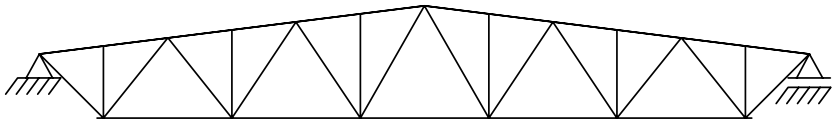

(c) KT-truss.

Figure 2.2: *Truss topologies.*

Connections between columns and foundation are considered rigid in the plane of the frame. Chords are connected to the columns with a hinge. Connection at the peak of the top chord is rigid. Three different truss types considered in this study are: N-, K- and KT-trusses. These topologies are described in Fig. 2.2.

The advantage of K-truss is the smallest number of braces compared to other two types. On the other hand, buckling length of top chord is bigger because the chord is not as densely supported as in other two truss types. KT-truss is therefore more suitable when the span of the truss is longer. The disadvantage of the KT-truss is the large number of members and joints. The joints of KT-truss can also be difficult to design. The idea of N-truss is that compressed vertical brace members are shorter than in other truss types.

2.1 Structural analysis

Both chords and columns are modeled and analyzed as continuous beams. Upper chord is under compression and bending. On the other hand lower chord is under tension and bending. Brace members are only under axial force. Braces are considered as pin-connected to the chords. Columns are modeled with two members. The first member is modeled from foundation to bottom chord and the second part from bottom chord to top chord.

The structure to be studied is hyperstatic so structural analysis is carried out by

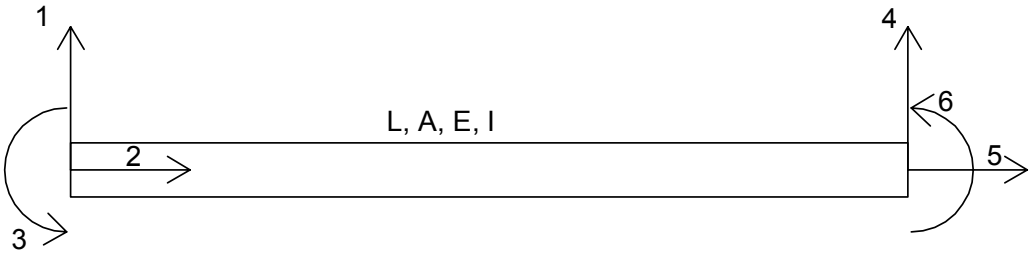

Figure 2.3: *Simple linear beam element in plane.*

using *finite element method* (FEM). Elements are simple linear beams which have 6 degrees of freedom in plane. This beam element is shown in Fig. 2.3. The rotational degrees are disregarded in braces because they are pin-connected to the chords. Each member of the frame is modeled with one element.

Linear static analysis is performed by using system of equations that can be written in the form

$$\mathbf{K}\mathbf{u} = \mathbf{F} \tag{2.1}$$

where global stiffness matrix $\mathbf{K}$ is constructed from corresponding element matrices $\mathbf{k}$ and $\mathbf{F}$ is global load vector. Global stiffness matrix $\mathbf{K}$ does not depend on nodal displacements $\mathbf{u}$ in linear case. Therefore nodal displacements can be solved by multiplying the equation with the inverse matrix

$$\mathbf{u} = \mathbf{K}^{-1}\mathbf{F} \tag{2.2}$$

Based on these displacements, it is possible to calculate the internal forces acting on both ends of the element. These internal forces include normal force N, bending moment M and shear force V.

Structural analysis must take into account the possible effects on the structure caused by the eccentricities of the joints. Large eccentricities may cause undesirable additional bending moments to the chord. In the design of joints, the important aspect is also to choose the type of joint. There are two possible joint types for the joints where more than one brace is connected to the chord. These two joint types are gap joints and overlap joints which are shown in Fig. 2.4.

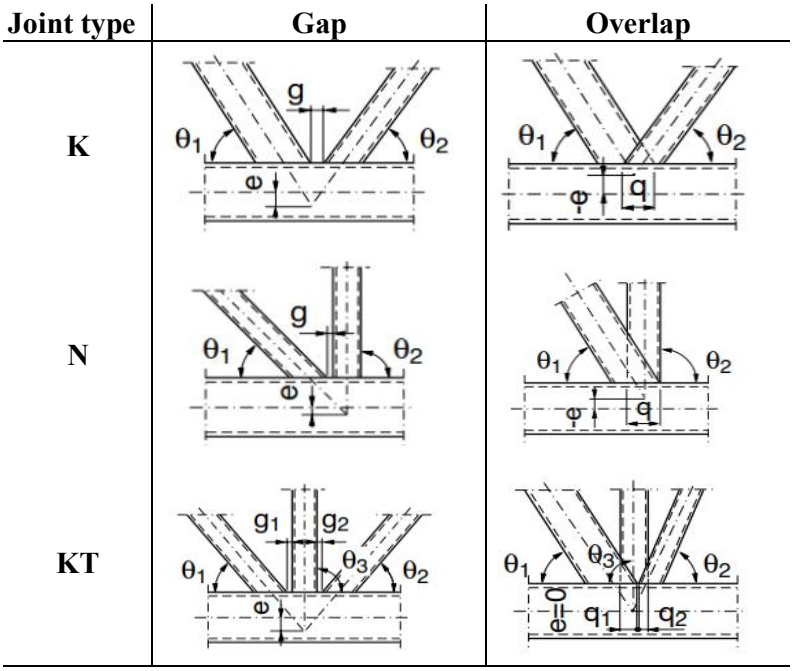

Figure 2.4: *Dimensions of joints with gap or overlap.*

The cutting of the brace ends and the joint welding in workshop are easier for the gap joints making it cheaper option than overlap joints. On the other hand, the strength of overlap joint is usually better because eccentricities are easier to minimize than in gap joints. In this thesis, only gap joints are considered. EN 1993-1-8 [12] presents minimum and maximum values for the gap g. These geometrical demands are introduced later in subsection 2.2.5.

The eccentricity e can be ignored in the design of joints, brace members and tensioned chord if the following condition is met

$$-0.55 \leq \frac{e}{h_0} \leq 0.25 \tag{2.3}$$

where h_0 is the cross-section height of the chord. In the design of compressed chord the additional bending moments have to be always taken into account. The moments are divided to both sides of the connection to compressed chord members in proportion to their relative rigidity I/L.

In this thesis eccentricities are modeled with short and stiff elements which are connected from the point where brace meets the surface of chord to the center line of the chord. Profile of these eccentricity elements is IPE 500 which is a very rigid cross-section. Fig. 2.5 illustrates how these elements are created in FE-model.

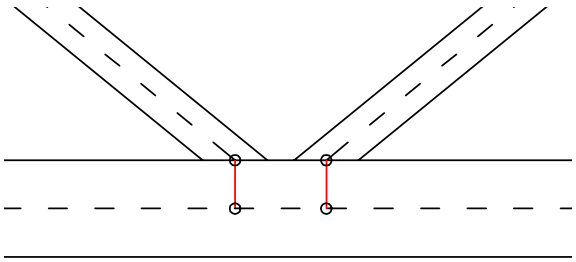

Figure 2.5: *Eccentricity elements in FE-model with pinned joints.*

Chords are modeled in the joint area so that a short separate stub element is modeled between the eccentricity elements in the gap area. These stub elements are similar compared to other chord elements.

2.2 Design code requirements

A safe and reliable steel frame has to satisfy criteria of the relevant design code. Design rules include member and joint strength, stability, geometrical restrictions of joints, serviceability and fire design. In this thesis serviceability and fire design are excluded. Also stability is considered only for individual members. In practical design the stability of the whole building should also be checked.

This thesis concentrates on SHS profiles and the following equations apply to those profiles. However, the next design principles apply to other steel profiles as well. Design rules presented in this section are based on Eurocode 3 [11, 12].

2.2.1 Cross-section classification

Cross-sections are classified to different classes in Eurocode 3. The purpose of classification is to determine how much local buckling limits the strength and deformation capacity of the cross-section. Cross-sections are divided into 4 different classes based on the slenderness of compressed parts. Class 1 sections can form a plastic hinge with the rotation capacity required from plastic analysis without the need to reduce cross-section capacity. In class 2 plastic bending capacity can be used, but local buckling limits the rotation capability.

In this study only classes 1 and 2 are used for all the members of portal frame. This requirement comes from the geometry rules of welded joints in Eurocode 3. EN 1993-1-1 Table 5.2 [11] presents the maximum width-to-thickness ratios for compressed parts in different classes. Maximum ratio for class 2 is

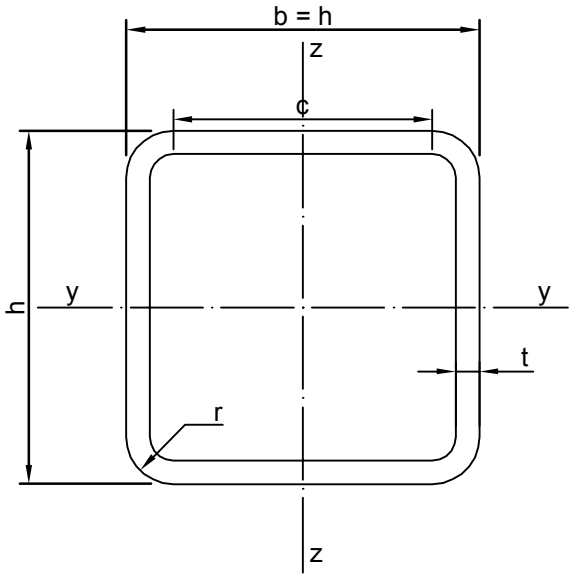

Figure 2.6: *Cross-section of SHS profile.*

$$\frac{c}{t} \leq 38\epsilon \tag{2.4}$$

where $\epsilon = \sqrt{235/f_{\mathrm{y}}}$. f_{y} is yield strength of the steel. Parameter c depends on cross-sectional dimensions presented in Fig. 2.6.

2.2.2 Member strength

The strength of each individual member of the frame should be evaluated. The cross-section capacity should be sufficient for axial force (tension or compression), bending and shear.

Design criterion for tension is

$$N_{\mathrm{t,Ed}} \leq N_{\mathrm{pl,Rd}} \tag{2.5}$$

where $N_{\mathrm{t,Ed}}$ is design tension force and $N_{\mathrm{pl,Rd}}$ is design axial capacity. Respectively the criterion for compression without buckling is

$$N_{\mathrm{c,Ed}} \leq N_{\mathrm{pl,Rd}} \tag{2.6}$$

where $N_{c,Ed}$ is design compression force. The design plastic axial capacity is calculated using the total area of cross-section A and yield strength f_y

$$N_{pl,Rd} = \frac{Af_y}{\gamma_{M0}} \tag{2.7}$$

where partial safety factor is $\gamma_{M0} = 1.0$.

The design criterion for bending in the plane of the frame is

$$M_{Ed} \leq M_{c,Rd} \tag{2.8}$$

where M_{Ed} is the design bending moment. The design bending capacity $M_{c,Rd}$ can be calculated by plastic theory in cross-section classes 1 and 2

$$M_{c,Rd} = M_{pl,Rd} = \frac{W_{pl}f_y}{\gamma_{M0}} \tag{2.9}$$

where W_{pl} is the plastic section modulus. The design bending capacity must be reduced if axial force exceeds following limit values. The formula for the bending capacity taking into account axial force is written in form

$$M_{N,Rd} = \begin{cases} M_{pl,Rd} & \text{if } N_{Ed} \leq \min\left(\dfrac{0.5(A-2bt)f_y}{\gamma_{M0}}, 0.25N_{pl,Rd}\right) \\ \min\left(M_{pl,Rd}\dfrac{1-n}{1-0.5a_w}, M_{pl,Rd}\right) & \text{otherwise} \end{cases} \tag{2.10}$$

Factors for Eq. (2.10) are

$$n = N_{Ed}/N_{pl,Rd}$$
$$a_w = \min((A-2bt)/A, 0.5)$$

For shear force the design criterion is as follows

$$V_{Ed} \leq V_{pl,Rd} \tag{2.11}$$

Shear capacity is calculated according to plastic theory

$$V_{\mathrm{pl,Rd}} = \frac{A_v f_{\mathrm{y}}}{\sqrt{3}\gamma_{\mathrm{M0}}} \tag{2.12}$$

where the shear area of SHS profile is

$$A_v = \frac{Ah}{b+h} \tag{2.13}$$

2.2.3 Buckling

The design criterion (2.6) for compression is seldom decisive criterion in dimensioning of the compressed member. Especially when lengths of compressed members are long, buckling is the prevailing phenomenon. Criterion for buckling should satisfy

$$N_{\mathrm{c,Ed}} \leq N_{\mathrm{b,Rd}} \tag{2.14}$$

This criterion must be verified in both directions: in the plane of the frame and out of the plane. Design value of buckling strength is in section classes 1-3

$$N_{\mathrm{b,Rd}} = \frac{\chi A f_{\mathrm{y}}}{\gamma_{\mathrm{M1}}} \tag{2.15}$$

and partial safety factor for buckling is $\gamma_{\mathrm{M1}} = 1.0$. Reduction factor χ is

$$\chi = \min\left(\frac{1}{\Phi + \sqrt{\Phi^2 - \bar{\lambda}^2}}, 1.0\right) \tag{2.16}$$

where

$$\Phi = 0.5(1 + \alpha(\bar{\lambda} - 0.2) + \bar{\lambda}^2) \tag{2.17}$$

For cold formed structural hollow sections imperfection factor $\alpha = 0.49$ is used. Furthermore the non-dimensional slenderness is in section classes 1-3

$$\bar{\lambda} = \frac{L_{cr}}{\pi i}\sqrt{\frac{f_{\mathrm{y}}}{E}} \tag{2.18}$$

where elastic modulus is $E = 210$ GPa and i is radius of gyration. If $\bar{\lambda} \leq 0.2$ then buckling can be ignored and it is sufficient to check only Eq. (2.6) for compression. The following buckling lengths are applied for members where L is distance between nodes: $L_{cr} = 0.9L$ for chords both in and out of the plane, $L_{cr} = 0.75L$ for braces both in and out of the plane and $L_{cr,y} = 1.2L$ for columns in plane and $L_{cr,z} = 1.0L$ out of the plane. Buckling lengths of chords and braces are chosen according to EN 1993-1-1 and its national annex [8, 11]. The buckling lengths of column are approximated by assuming that the truss supports columns in the plane of the frame. Out of the plane columns are considered to be hinge-supported at both ends.

In combined bending and axial compression a frame member should satisfy equations

$$\frac{N_{\mathrm{c,Ed}}}{\chi_{\mathrm{y}} \frac{N_{\mathrm{Rk}}}{\gamma_{\mathrm{M1}}}} + k_{yy} \frac{M_{\mathrm{Ed}}}{\chi_{\mathrm{LT}} \frac{M_{\mathrm{Rk}}}{\gamma_{\mathrm{M1}}}} \leq 1 \tag{2.19}$$

$$\frac{N_{\mathrm{c,Ed}}}{\chi_{\mathrm{z}} \frac{N_{\mathrm{Rk}}}{\gamma_{\mathrm{M1}}}} + k_{zy} \frac{M_{\mathrm{Ed}}}{\chi_{\mathrm{LT}} \frac{M_{\mathrm{Rk}}}{\gamma_{\mathrm{M1}}}} \leq 1 \tag{2.20}$$

where

$N_{\mathrm{Rk}} = A f_{\mathrm{y}}$
$M_{\mathrm{Rk}} = W_{\mathrm{pl}} f_{\mathrm{y}}$
χ_{y} and χ_{z} are reduction factors calculated separately for y- and z-axis
$\chi_{\mathrm{LT}} = 1$ is reduction factor for lateral-torsional buckling

Interaction factors k_{yy} and k_{zy} for SHS profiles are calculated so that

$$k_{yy} = C_{my} \min \left(1 + (\bar{\lambda} - 0.2) \frac{N_{\mathrm{c,Ed}}}{\chi_{\mathrm{y}} N_{\mathrm{Rk}} / \gamma_{\mathrm{M1}}}, 1 + 0.8 \frac{N_{\mathrm{c,Ed}}}{\chi_{\mathrm{y}} N_{\mathrm{Rk}} / \gamma_{\mathrm{M1}}} \right) \tag{2.21}$$

$$k_{zy} = 0.6 k_{yy} \tag{2.22}$$

Equivalent uniform moment factor C_{my} can be defined with the help of a bending moment diagram. In this thesis conservative assumption $C_{my} = 1$ is applied.

2.2.4 Geometry of welded joints

The simplest way to connect structural hollow sections is welding. Each welded joint has to meet certain demands so that joint resistance formulas presented in EN 1993-1-8 [12] are valid. The geometry of joint has to satisfy following constraint for each brace member and chord

$$\frac{h}{t} \leq 35 \tag{2.23}$$

For SHS profiles criterion $0.5 \leq h/b \leq 2.0$ is always satisfied since the height and the width of cross-section are same. The brace side lengths h_b must also be at least 35% of the chord side lengths h_0 in K/N-joints. Eurocode 3 does not provide upper limit for the side lengths of braces but in this study, the brace side lengths are limited to 35-85% of the chord side lengths to facilitate welding.

$$0.35h_0 \leq h_b \leq 0.85h_0 \tag{2.24}$$

2.2.5 Strength of joints

In this thesis, only welded truss joints are included in the optimization problem. Pinned chord-to-column connections and rigid column-base connections are not treated.

Joints between chord and brace members are assumed to be pure hinge joints and brace members are designed only with respect to the normal force. The joint strengths are expressed as a maximum allowed normal force that can act on a brace member:

$$N_{\mathrm{Ed,i}} \leq N_{\mathrm{Rd,i}} \tag{2.25}$$

Dimensions and symbols of K/N- and KT-joints are presented in Fig. 2.7. Subscript 0 refers to the chord and subscripts 1 and 2 to the braces. Brace 1 is under compression and brace 2 under tension. Third brace member in the middle of KT-joint is marked with subscript 3. To ensure weldability of the joint the minimum joint angle θ_i between brace and chord is 30 °, the minimum wall thickness is 2.5 mm and eccentricity e has to fulfill criterion (2.3).

Eccentricity and joint gap depend on each other so that

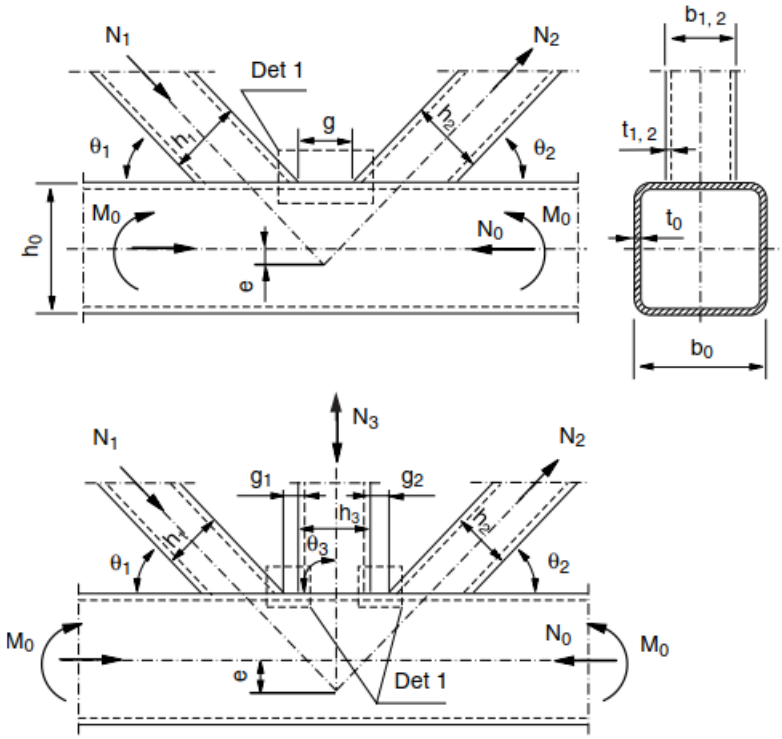

Figure 2.7: *Dimensions and symbols of K/N- and KT-joints with gap [26].*

$$e = \frac{\sin\theta_1 \sin\theta_2}{\sin(\theta_1 + \theta_2)}\left(g + \frac{h_1}{2\sin\theta_1} + \frac{h_2}{2\sin\theta_2}\right) - \frac{h_0}{2} \tag{2.26}$$

During the optimization the gap size $g = 30$ mm is assumed. The eccentricity is minimized in the FE-model before and after optimization so that gap size meets the demands presented in EN 1993-1-8 [12]

$$max(t_1 + t_2,\, 0.5b_0(1-\beta)) \leq g \leq 1.5b_0(1-\beta) \tag{2.27}$$

In the case of KT-joint gaps g_1 and g_2 must be both checked separately. Parameter β is calculated for the K/N-joints with following formula

$$\beta = \frac{b_1 + b_2}{2b_0} \tag{2.28}$$

The joint failure modes which may occur depend on type, geometry and loads of the joint. N-, K-, KT- and Y-joints are studied in this thesis. Fig. 2.8 presents possible

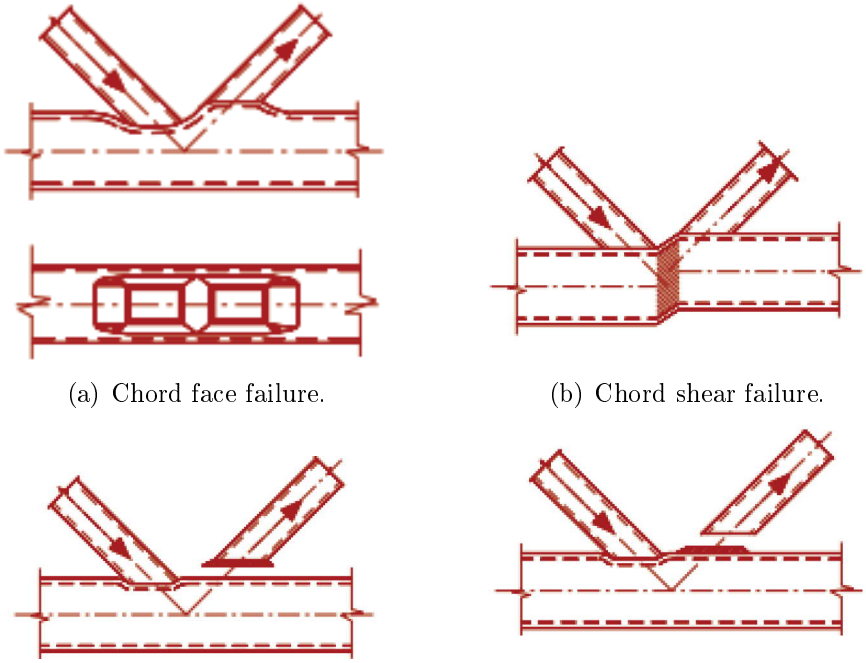

(a) Chord face failure.

(b) Chord shear failure.

(c) Punching shear failure of chord.

(d) Brace failure.

Figure 2.8: *Failure modes of joints between SHS profiles [12].*

failure modes for N- and K-joints.

As mentioned earlier, the capacities of these failure modes are expressed as a maximum allowed normal force in a brace member. The capacities of K/N-joints with gap are calculated with following equations

$$N_{\mathrm{Rd,i}} = \frac{8.9 k_{\mathrm{n}} f_{\mathrm{y0}} t_0^2 \sqrt{\gamma}\beta}{\sin\theta_{\mathrm{i}}} / \gamma_{\mathrm{M5}} \quad \text{Chord face failure} \tag{2.29}$$

$$N_{\mathrm{Rd,i}} = \frac{f_{\mathrm{y0}} A_v}{\sqrt{3}\sin\theta_{\mathrm{i}}} / \gamma_{\mathrm{M5}} \quad \text{Chord shear} \tag{2.30}$$

$$N_{Rd,0} = \left((A_0 - A_v) f_{\mathrm{y0}} + A_v f_{\mathrm{y0}} \sqrt{1 - (V_{\mathrm{Ed}}/V_{\mathrm{pl,Rd}})^2} \right) / \gamma_{\mathrm{M5}} \quad \text{Chord shear} \tag{2.31}$$

$$N_{\mathrm{Rd,i}} = f_{\mathrm{yi}} t_{\mathrm{i}} (2h_{\mathrm{i}} - 4t_{\mathrm{i}} + b_{\mathrm{i}} + b_{eff}) / \gamma_{\mathrm{M5}} \quad \text{Brace failure} \tag{2.32}$$

$$N_{\mathrm{Rd,i}} = \frac{f_{\mathrm{y0}} t_0}{\sqrt{3}\sin\theta_{\mathrm{i}}} \left(\frac{2h_{\mathrm{i}}}{\sin\theta_{\mathrm{i}}} + b_{\mathrm{i}} + b_{\mathrm{e,p}} \right) / \gamma_{\mathrm{M5}} \quad \text{Punching shear if } \beta \leq (1 - 1/\gamma) \tag{2.33}$$

Dimensions h_0, h_{i}, b_0, b_{i}, t_0, t_{i} and angles θ_i are presented in Fig. 2.7. f_{y0} and f_{yi} are yield strengths of chord and braces. Safety factor of joints is $\gamma_{\mathrm{M5}} = 1.0$. Parameter γ depends on chord dimensions

$$\gamma = 0.5 b_0 / t_0 \tag{2.34}$$

Formula for k_n is

$$k_\mathrm{n} = \begin{cases} 1.0 & \text{tension chord} \\ \min\left(1.3 - \dfrac{0.4|n|}{\beta}, 1.0\right) & \text{compression chord} \end{cases} \tag{2.35}$$

where n is calculated for compressed chord with equation

$$n = \frac{N_{0,\mathrm{Ed}}}{A_0 f_{\mathrm{y}0} / \gamma_{\mathrm{M5}}} + \frac{M_{0,\mathrm{Ed}}}{W_{\mathrm{el},0} f_{\mathrm{y}0} / \gamma_{\mathrm{M5}}} \tag{2.36}$$

$N_{0,\mathrm{Ed}}$ is larger of absolute values of chord normal force (left or right side of joint). $M_{0,\mathrm{Ed}}$ is the bending moment of the joint. A_0 and $W_{\mathrm{el},0}$ are cross-section area and elastic section modulus of chord. A_v is the shear area of chord

$$A_v = (2h_0 + \alpha b_0) t_0 \tag{2.37}$$

where

$$\alpha = \sqrt{\frac{1}{1 + \dfrac{4g^2}{3t_0^2}}} \tag{2.38}$$

Furthermore, V_{Ed} is chord shear at gap area. Effective widths for brace failure and chord face punching shear are as follows

$$b_{eff} = \min\left(\frac{10 t_0^2 f_{\mathrm{y}0} b_\mathrm{i}}{b_0 f_{\mathrm{y}i} t_\mathrm{i}}, b_\mathrm{i}\right) \tag{2.39}$$

$$b_{\mathrm{e,p}} = \min\left(\frac{10 t_0 b_\mathrm{i}}{b_0}, b_\mathrm{i}\right) \tag{2.40}$$

In the case of KT-joints the resistances of all three braces should be checked. KT-joint is calculated by dividing the joint into two K/N-joints. Braces 1 and 2 are calculated as K-joint (Fig. 2.7). Vertical brace is assumed to form N-joint with

either brace 1 or 2. If the vertical is under tension then its pair is the compressed brace 1. Respectively, when the vertical is under compression it forms a pair with tensioned brace 2.

In the case of Y-joint, the possible failure modes are chord face failure, chord side wall buckling, chord face punching shear or brace failure. The choice of the relevant failure mode depends on parameter $\beta = b_\mathrm{i}/b_0$. In this thesis side lengths of braces are limited to a maximum of 85% of chord side lengths. When $\beta \leq 0.85$ the only possible failure type is the chord face failure. The resistance formula for the chord face failure in the case of Y-joint is according to EN 1993-1-8 table 7.11 [12]

$$N_{\mathrm{Rd,i}} = \frac{k_\mathrm{n} f_{\mathrm{y}0} t_0^2}{(1-\beta)\sin\theta_\mathrm{i}} \Big(\frac{2\eta}{\sin\theta} + 4\sqrt{(1-\beta)} \Big) / \gamma_{\mathrm{M5}} \tag{2.41}$$

where $\eta = h_\mathrm{i}/h_0$ and parameter k_n is calculated with Eqs. (2.35) and (2.36).

The steel grade is taken into account for joint resistances. The above-mentioned resistances are reduced with a reduction factor when high strength steel is used in the members of the joint. In this thesis, reduction factor 1.0 is chosen for steel grades S355 and S420. Factor 0.9 is applied when steel grade is S700. These choices are based on proposed values presented in [14].

3. OPTIMIZATION METHOD

Various optimization methods and algorithms have been studied for problems of structural optimization [6, 16, 20, 22, 30]. The profile selection and constraints formed on the basis of Eurocode 3 lead to a discrete, nonlinear and nonconvex optimization problem. This limits the number of possible solution methods. Methods that use derivation of the objective and constraint functions may get caught in the local minimum in these kind of problems.

Arora & Huang have presented four different approaches for solving this kind of a problem [3]. Simplest and fastest of these approaches is called rounding-off method. In this method discrete problem is first relaxed into continuous problem and solved by some gradient-based method. Then the final discrete solution is sought from the neighborhood of continuous solution. This two-stage procedure usually leads to conservative result compared to methods that use full design space. It should be noted that the global optimum of the discrete problem is not necessarily located near the result of the continuous problem.

The speed and efficiency of the two-stage procedure and direct optimization have been previously compared with tubular truss in [31]. Direct optimization means a method where the optimization is done with the full design space instead of narrowing the design space first by relaxing the problem as continuous and finding a solution for the continuous problem. In the case of tubular truss two-stage procedure proved to be much faster and more efficient. The purpose of this study was to search for a method that is able to find a good solution within an appropriate time. Therefore two-stage procedure was chosen although it does not guarantee finding a global optimum.

There are two cases studied in this thesis regarding optimization of brace members. The simplest way to formulate portal frame optimization problem is to keep the same profile for every brace. This makes totally 8 different optimization variables for the frame: cross-sectional heights and wall thicknesses of column, chords and braces. However, it is beneficial to allow braces to have different profiles since their internal forces vary significantly. The outermost braces in the truss are much more

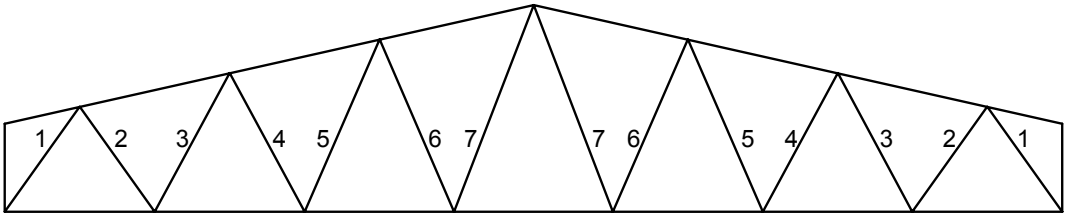

Figure 3.1: *Symmetry pairs of the roof truss.*

heavily loaded compared to braces in the middle of the truss.

Symmetrical shape of the truss is exploited in brace optimization. Braces are divided into symmetrical pairs as shown in Fig. 3.1. Optimization of symmetry pairs is done after the optimization of the whole frame where braces are considered to be same profile. Forcing the braces to be same profile at first reduces calculation time because number of variables is much smaller. It is also assumed that changing the brace profiles does not have an impact on utilization rates of chords and columns. Therefore chord and column profiles can be fixed to match the result of the first problem where braces are assumed to be same profile. In the second problem, only symmetry pairs of braces are optimized while the profiles of other members of the frame are already decided. This strategy will ultimately lead to a four-stage optimization procedure because two different problems are both solved in two stages.

3.1 Continuous problem

3.1.1 Interior-point algorithm

In the first stage of the optimization the design variables are treated as continuous. In continuous problem the variables can have any kind of value from the certain value range. The continuous problem is solved by using *'interior-point'* -algorithm in MATLAB. This gradient-based algorithm is useful for solving continuous and nonlinear problems. Interior-point algorithm requires a starting point for optimization which is given by user. The starting point is an initial guess for the solution.

Derivatives are approximated by finite differences during optimization of the continuous problem. Interior-point algorithm uses a forward difference as default in MATLAB. The derivative of function f at the point x is expressed as

$$f'(x) = \frac{f(x+h) - f(x)}{h} \tag{3.1}$$

In this thesis the variables x_j are gathered into the vector $\mathbf{x}$ so the derivatives are calculated by components.

Due to the nature of the problem interior-point algorithm can not guarantee finding the global minimum. The problem is non-convex and highly nonlinear which may cause difficulties for the algorithm. For this reason, the quality of the starting point has a great impact on the solution. It is possible that algorithm does not find any feasible solution near the starting point or stops at local minimum. Therefore several different starting points should be used in order to ensure the quality of the solution. In this study, the first continuous problem is solved 10 times by using different starting point each time. The second problem is solved only once by using the previous discrete solution as a starting point.

The time requirement for solving the whole problem is also taken into consideration in the options of the algorithm. Due to large size of the problem, the algorithm may converge very slowly. For this reason, a maximum limit for 500 function evaluations is set for the continuous problem. The time taken for function evaluation depends largely on implementation. With the MATLAB -implementation used in this thesis, one function evaluation takes from 0.12 to 0.17 seconds depending on the frame to be optimized. This means a time limit of approximately one minute for solving a continuous problem with one starting point.

3.1.2 Starting point selection

When choosing starting points one must also note that interior-point algorithm requires the starting point to be feasible. Thus, a separate method needs to be developed for the selection of starting points to avoid infeasible points. The upper bounds of the variables presented in Section 4.1 are selected as the first starting point. This starting point can safely be assumed to be located in the feasible region also taking into account the joint geometry. The other nine points are generated based on loads and geometry of the frame. The roof truss is assumed to be a single-span beam. The maximum bending moment and vertical support forces of the beam are then calculated with following formulas

$$M_{beam} = \frac{(p_1 + p_2)L^2}{8} \tag{3.2}$$

$$V_{beam} = \frac{(p_1 + p_2)L}{2} \tag{3.3}$$

where p_1, p_2 and L are introduced in Fig. 2.1. Then the maximum normal force of top chord is estimated by using height of the truss as beams tension indicator

$$N_{beam} = \frac{M_{beam}}{H_3} \tag{3.4}$$

Top chord profiles are chosen based on this estimated force. Utilization rate of axial resistance of top chord is assumed to be 40% and so the estimated cross-section area of the top chord is obtained from equation

$$A_{0,est} = \frac{N_{beam}}{0.4 f_{y0}} \tag{3.5}$$

This estimated area $A_{0,est}$ is compared to 60 different SHS profiles that have side lengths between 100-300 mm and wall thicknesses between 4-12.5 mm. Among these 60 options, nine profiles that have cross-section area closest to the estimated area are selected as starting points for top chord. Bottom chord profiles are then selected so that their side length and wall thickness are 85% of the corresponding top chord profile dimensions. Furthermore, brace profile dimensions are 85% of the corresponding bottom chord profile.

At the same time starting points for column profile are selected according to the estimated normal force and bending moment of the column. The support reaction of the beam V_{beam} is taken as normal force of the column. Columns and truss form a rigid frame so the bending moment of the column is estimated according to formulas for a simplified frame presented in Fig. 3.2.

Bending moment is estimated at the right bottom corner of the frame (point D in Fig. 3.2.) Bending moment from horizontal loads is calculated by

$$M_{col,h} = \frac{(p_1 + p_2)L^2}{12N_1} \tag{3.6}$$

Bending moment caused by the wind loads is estimated by

$$M_{col,v} = \frac{H_1^2}{4}\left(q_1\Big(-\frac{k+3}{6N_1} + \frac{4k+1}{N_2}\Big) - q_2\Big(-\frac{k+3}{6N_1} - \frac{4k+1}{N_2}\Big)\right) \tag{3.7}$$

where coefficients are $N_1 = k + 2$ and $N_2 = 6k + 1$. Parameter k depends on both geometry of the frame and on the ratio between moments of inertia of the column

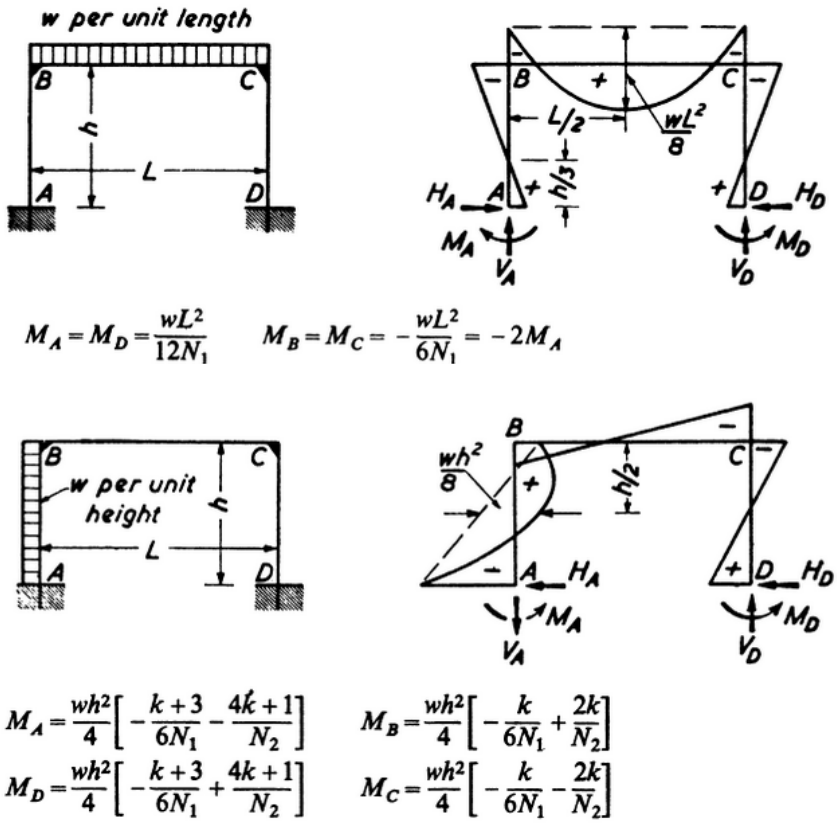

Figure 3.2: *Bending moments of the rigid frame with uniform loads [7].*

and beam. For calculating this ratio, cross-sections of column and truss members are required which naturally are not known before optimization. Here, ratio is assumed to be 60. This approximation is chosen on the basis of optimum solutions. Thus, parameter k is calculated by following estimation

$$k = 60\frac{H_1}{L} \tag{3.8}$$

Finally the cross-section is estimated by calculating combined stress of bending and axial force

$$\sigma = \frac{(M_{col,h} + M_{col,v})}{W_{\text{el}}} + \frac{V_{beam}}{A} \tag{3.9}$$

The selection of the column profile uses the same set of 60 SHS profiles as in selection of top chord profile. Nine alternatives are chosen from this set where combined stress is closest to 50% of the column yield limit. The utilization is set this small because the buckling of column is not taken into account in the above formula.

3.2 Discrete problem

3.2.1 Genetic Algorithm

In the second stage of the optimization problem the variables are changed from continuous to discrete. Discrete problem is solved by *Genetic Algorithm* which is implemented in MATLAB. GA is a heuristic population-based algorithm that imitates the principles of natural selection. It can not guarantee global minimum, but it can find a sufficient solution within reasonable time. GA is relatively general heuristic method that has been studied extensively in the field of structural optimization. It was first introduced in the 1970's [21].

GA is well suited for discrete optimization problems which are discontinuous or highly nonlinear. Its operating principle is based on a population consisting of individual solutions. GA repeatedly modifies these individuals as the optimization proceeds. At each step, GA selects certain individuals to be parents for the next generation. As generations evolve during the optimization, the algorithm approaches towards the optimum solution.

GA creates an initial population of possible solutions in the beginning of optimization. Population size means the number of individuals in each generation. A large population size means a more extensive search in the design space. On the other hand, this may also cause the calculation time to grow too high. Therefore, the user is responsible for determining the appropriate size. In this study population size is $n_{\text{pop}} = \min(8n_{\text{var}}, 200)$, where n_{var} is the number of variables.

The optimization proceeds so that the fitness score of each individual is evaluated after creating the new generation. Fitness score means the quality of an individual. It is assessed based on the objective value taking into account constraint violations. These fitness values will be used to create the next generation. The individuals with the highest fitness values are directly selected for the next generation. These best individuals are called *elite children.*

In addition to elite children, also two other types of children are considered when creating the new generation. *Mutation children* are produced by randomly altering the individual's properties. This prevents homogeneous population. In other words, mutation guarantees more thorough search in the design space. Mutation occurs with a certain probability that can be adjusted from the algorithm settings. Default value of 0.01 is used here.

Third type of the children are called *crossover children.* These are created by com-

bining two individuals to create a new individual from these parents. There are different kind of methods for producing crossover children. Default setting is used here which creates a random binary vector. Based on this vector the genes of two parents are transferred to the child. For example, if parents are $p_1 = \{a, b, c, d, e, f, g, h\}$ and $p_2 = \{i, j, k, l, m, n, o, p\}$ and binary vector is $\{1, 1, 1, 0, 0, 0, 1, 0\}$ then the child will be $c = \{a, b, c, l, m, n, g, p\}$.

GA continues to optimize for as long as one of the predefined stopping criteria is met. The user can define stopping criteria for example by setting a limit for the number of generations, optimization time or objective function value. In this thesis, maximum optimization time is set to one minute. This means that optimization is terminated when this time limit is reached.

3.2.2 Discrete neighborhood

Available profiles are chosen from the SSAB Domex Tube and Strenx Tube SHS-catalogs. Only profiles which are either cross-section class 1 or 2 are considered. Profiles are chosen based on the result of continuous optimization. For columns and chords three closest values compared to both side length and wall thickness are searched from profile catalog. For example, if the continuous result for top chord profile is SHS 160.17 x 6.81, then picked values for the side length are 150, 160 and 180 mm. Respectively, chosen values of wall thicknesses are 6, 7.1 and 8 mm. This makes total $3x3 = 9$ different profiles. This selection method is described in Fig. 3.3. For braces only two closest values are selected making it total $2x2 = 4$ profiles.

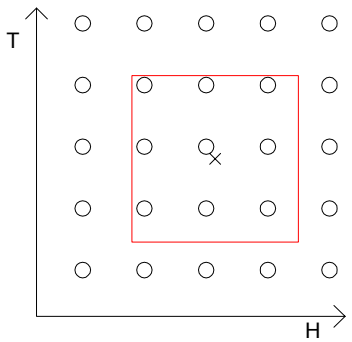

Figure 3.3: *The formation of discrete neighborhood. Cross indicates the continuous result and circles are available profiles near the result. Profiles inside the red square are selected.*

This selection method allows to include also smaller profiles into problem compared to continuous result. The above-mentioned example has SHS 160x6 as one possible profile. This profile is smaller than continuous result, but changing the profiles of

whole structure can affect internal forces so that this smaller profile becomes feasible. Also utilization rates in continuous result may not be full 100% so it is justified to include smaller profiles to profile selection.

This presented selection method makes totally 2916 different solutions for the first problem where the same profile is assumed for all brace members. It would take about 6-8 minutes for all options to be evaluated since one evaluation takes 0.12-0.17 seconds, depending on the structure being studied. In brace optimization the number of possible solutions is $4^{n_{sym}}$, where n_{sym} is the number of symmetry pairs.

3.3 Summary of optimization process

The whole optimization process includes four stages. The first two stages are continuous and discrete problem when braces are considered to be same profile. The third and fourth stages are continuous and discrete problem when symmetry pairs are taken into account. This whole process is described in Fig. 3.4.

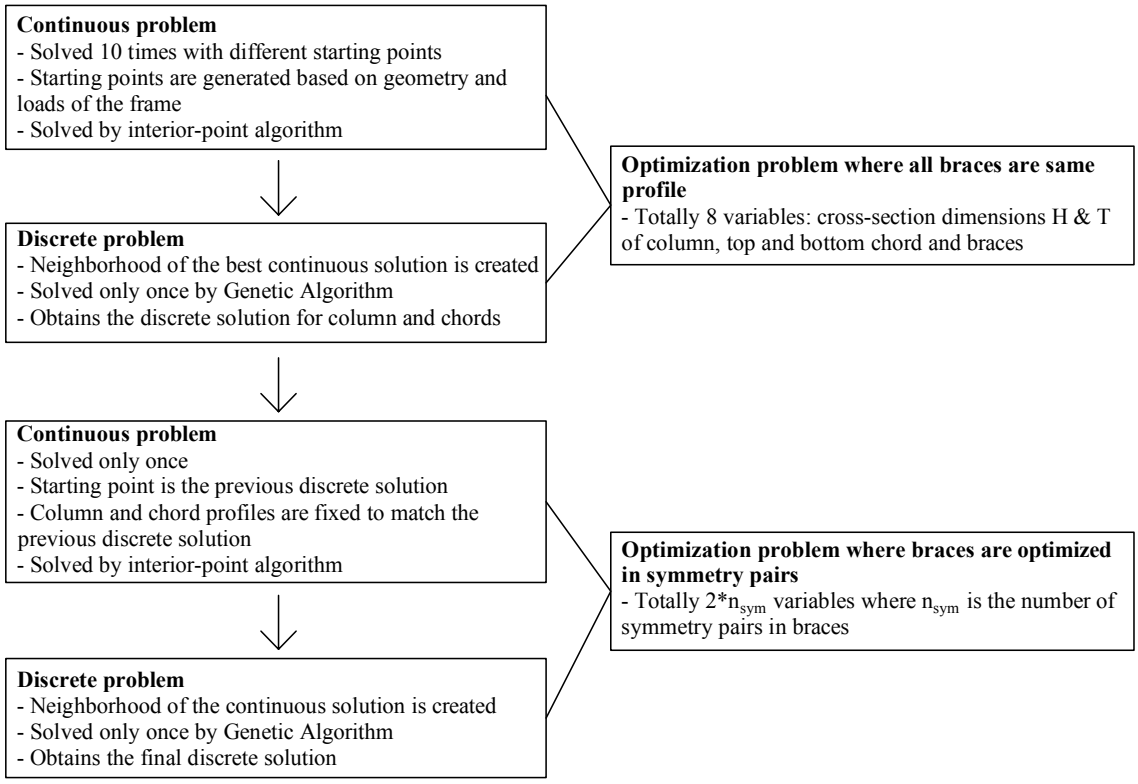

Figure 3.4: *Optimization process.*

During the optimization finite element model of the frame is constantly reconstructed. Fig. 3.5 demonstrates how the FE-model is updated during the optimization.

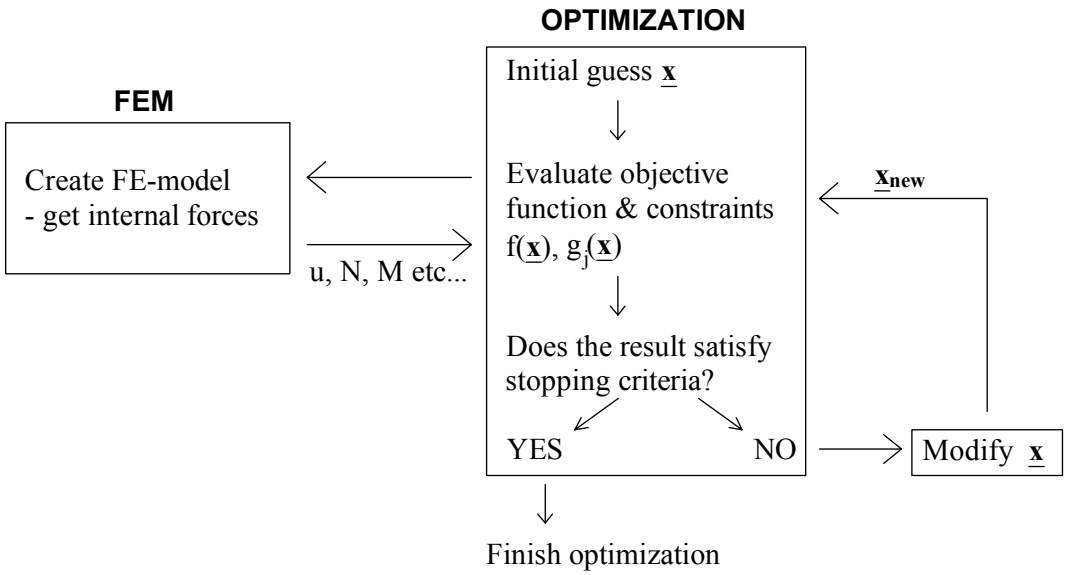

Figure 3.5: *Updating the FE-model of the frame during optimization.*

At first user gives an initial guess $\mathbf{x}$ for continuous optimization. In discrete optimization the initial guess is not needed because GA creates the initial population randomly from discrete neighborhood. FE-model is created with variables $\mathbf{x}$ and objective function and constraints are evaluated. After this, the algorithm checks whether stopping criteria are fulfilled. If criteria are not met, then algorithm modifies $\mathbf{x}$. Before evaluating constraints again the FE-model of the structure is reconstructed with these new modified values $\mathbf{x}_{\text{new}}$ to update the internal forces of the structure. Objective function and constraint evaluations are then carried out once again. Algorithm repeats this iteration loop as long as some stopping criterion becomes active.

The construction of the FE-model could be done with some separate structural design program. In this thesis, also the construction of the FE-model is executed with MATLAB.

4. PORTAL FRAME OPTIMIZATION PROBLEM

This study concentrates on only sizing optimization. Shape and topology are already decided beforehand and the optimum profiles are searched for given structure and loads.

Formulation of an optimization problem requires an objective function, design variables and constraints. In this study the total mass and cost of a frame are the objective functions. Dimensions of cross-sections are treated as design variables and constraints are formed by design criteria based on Eurocode 3.

4.1 Design variables

The height/width and wall thickness of SHS profile shown in Fig. 2.6 are chosen as design variables. Portal frame consists of four different profiles: top chord, bottom chord, brace members and columns when the same profile is used in every brace member. Thus, the total number of design variables is 8 for the first optimization problem to be solved. The variables are gathered into vector

$$\mathbf{x} = \{h_{\mathrm{tc}}\, t_{\mathrm{tc}}\, h_{\mathrm{bc}}\, t_{\mathrm{bc}}\, h_{\mathrm{b}}\, t_{\mathrm{b}}\, h_{\mathrm{c}}\, t_{\mathrm{c}}\} \tag{4.1}$$

where h_{tc}, h_{bc}, h_{b} and h_{c} are cross-sectional side lengths of top chord, bottom chord, braces and columns. Respectively, t_{tc}, t_{bc}, t_{b} and t_{c} are wall thicknesses of the corresponding profiles.

In the second optimization problem the variables change. Column and chord profiles are fixed so the variable vector is then written in form

$$\mathbf{x} = \{h_{b1}\, t_{b1}\, h_{b2}\, t_{b2}\, \ldots\, h_{bn}\, t_{bn}\} \tag{4.2}$$

where the number of profiles is equal to the number of symmetry pairs $n = n_{sym}$.

Table 4.1: *Lower and upper bounds of variables.*

Bounds	**Top Chord** $h_{\mathbf{tc}}$**x** $t_{\mathbf{tc}}$**[mm]**	**Bottom Chord** $h_{\mathbf{bc}}$**x** $t_{\mathbf{bc}}$**[mm]**	**Braces** $h_{\mathbf{b}}$**x** $t_{\mathbf{b}}$**[mm]**	**Columns** $h_{\mathbf{c}}$**x** $t_{\mathbf{c}}$**[mm]**
Lower bound	100 x 4	80 x 4	50 x 3	100 x 4
Upper bound	300 x 12.5	200 x 10	150 x 8	300 x 12.5

Variables are treated as continuous in the first stage of optimization. Lower and upper bounds for continuous problem are determined for each variable in Table 4.1.

In the second stage of optimization where the discrete solution is searched, variables change from continuous to discrete. The discrete variables are specified with indices. Variable x_j can take values only from the set $S = v_1, \ldots, v_k$. This set is the discrete neighborhood. For column and chords the number of possible values is $k = 3$ and for braces $k = 2$. In discrete optimization x_j is treated as an integer variable taking values from 1 to k and $S(x_j)$ is the corresponding discrete value in the discrete neighborhood. Now the lower bound is 1 and the upper bound is k for each variable.

Transformed integer variables x_j are passed to the objective and constraint functions when GA-solver is called in MATLAB. In order to evaluate these functions correctly the variables x_j are transformed to the corresponding discrete values $S(x_j)$ before the evaluation.

4.2 Objective function

As mentioned earlier both minimum-mass and minimum-cost solutions are searched. Usually the mass of structure is used as objective function for simplicity because minimum-mass solution is often close to the most cost-effective solution. In more detail the costs are comprised of more than just material consumption. Also sawing, blasting, welding and painting affect the total cost.

Several different objective functions can be managed at the same time in optimization problem. This kind of approach is called multicriteria optimization. However, in this thesis single criterion optimization is used which means that mass and cost optimization are treated separately and the results are compared to each other.

4.2.1 Mass function

In mass minimization the objective function is the total mass of the structure. In this case formulation of objective function is fairly straightforward. The mass function

for the frame is

$$W(\boldsymbol{x}) = \rho \sum_{i=1}^{n_E} l_i A_i(\boldsymbol{x}) \tag{4.3}$$

where density of steel is $\rho = 7850 \cdot 10^{-9}$ kg/mm^3, n_E is a number of members in frame and l_i and A_i are the length and cross-sectional area of member i, respectively.

4.2.2 Cost function

There have been presented different kind of cost functions for steel structures in literature [18, 24, 28]. The cost functions used in this thesis are presented by Haapio [18]. These cost functions include productive and non-productive time. The labour, equipment, maintenance, real estate, energy and both time-related and non-time-related consumables are taken into account in cost functions.

In this study, only manufacturing costs are included in total costs. For instance, transportation and erection of the frame are omitted from calculations. All the constants and parameters are adopted from [18]. Thus, total cost function is presented as follows:

$$C(\boldsymbol{x}) = C_{\mathrm{M}}(\boldsymbol{x}) + C_{\mathrm{B}}(\boldsymbol{x}) + C_{\mathrm{S}}(\boldsymbol{x}) + C_{\mathrm{P}}(\boldsymbol{x}) + C_{\mathrm{PA}}(\boldsymbol{x}) \tag{4.4}$$

where

$C(\boldsymbol{x})$ is total cost [€]
$C_{\mathrm{M}}(\boldsymbol{x})$ is material cost [€]
$C_{\mathrm{B}}(\boldsymbol{x})$ is blasting cost [€]
$C_{\mathrm{S}}(\boldsymbol{x})$ is sawing cost [€]
$C_{\mathrm{P}}(\boldsymbol{x})$ is painting cost [€]
$C_{\mathrm{PA}}(\boldsymbol{x})$ is part assembling (welding) cost [€]

Material cost

Material cost of the frame is computed by

$$C_{\mathrm{M}}(\boldsymbol{x}) = \rho \sum_{i=1}^{n_E} c_{SM,i} l_i A_i(\boldsymbol{x}) \tag{4.5}$$

where c_{SM} is the unit cost of the profile [€/kg]. In this thesis only SHS profiles are used for frame members. For SHS profiles the unit cost $c_{SM} = 0.8$ [€/kg] is applied when steel grade is S355. The cost factors for stronger steel grades have been presented in [14]. In this thesis, test cases include grades S355, S420 and S700. The cost factor 1.3 is used for S700. Factor 1.075 is applied when the grade is S420.

Blasting cost

Blasting cost is comprised of labour, equipment, maintenance, real estate investment, consumables and energy consumption. The function for blasting cost is

$$C_{\mathrm{B}}(\boldsymbol{x}) = 3.63 \cdot 10^{-4} \sum_{i=1}^{n_E} l_i \tag{4.6}$$

The unit for constant $3.63 \cdot 10^{-4}$ is [€/mm].

Sawing cost

The ends of the each member are sawn. Sawing cost depends on the angles of the member ends. The ends of the members that are positioned diagonally in the frame must be bevelled. Sawing cost for member i is calculated by equation

$$C_{S,i} = (T_{NS} + T_{PS})c_S/u_S + T_{PS}(c_{CS} + c_{EnS}) \tag{4.7}$$

where T_{NS} is non-productive time, T_{PS} is productive time, c_{CS} is cost of sawing consumables, $c_S = 1.2$ [€/min] is constant that includes costs of labour, equipment, maintenance and real estate. $c_{EnS} = 0.02$ [€/min] is the cost of the energy. Utilization rate is $u_S = 1$.

The non-productive time [min] is defined in formula

$$T_{NS} = 4.5 + \lceil 1 - \cos\theta_1 \rceil + \lceil 1 - \cos\theta_2 \rceil + \frac{l_i}{20000} \tag{4.8}$$

Non-productive time includes the time for moving the profile and the blade, and also with the bevelled ends the rotating of the blade. θ_1 and θ_2 are the bevelling angles of the member ends. Term $\lceil 1 - \cos\theta_i \rceil$ is the ceiling function that returns the smallest integer that is greater than or equal to the argument. When the bevelling angle is $\theta_i = 0\,^\circ$, ceiling function returns the value $\lceil 1 - \cos\theta_i \rceil = 0$ because the end

is not bevelled. With any other value for the bevelling angle θ_i, the ceiling function returns $\lceil 1 - \cos\theta_i \rceil = 1$.

The productive time [min] is defined

$$T_{PS} = \frac{h_s}{S \cdot S_m} + \frac{A_h}{Q} \tag{4.9}$$

where the first term of the equation refers to the vertical parts of the cross-section and latter term refers to the horizontal parts. h_s is the sawing height of the vertical part. For SHS profiles the sawing height is calculated

$$h_s = h - 2r \tag{4.10}$$

Material factor S_m depends on steel grade so that $S_m = 0.9$ for S355 and $S_m = 0.8$ for stronger grades. Feeding speed [mm/min] is presented in continuous form

$$S = 0.0328t_{mv}^2 - 3.1794t_{mv} + 115.6 \tag{4.11}$$

where t_{mv} is thickness of the vertical part. In the case of bevelled cutting the thickness is $t_{mv} = t/\cos\theta$ with θ being the angle between the blade and the profile. For the horizontal parts the total sawing area is also dependent on the angle θ so that

$$A_h = \frac{2ht}{\cos\theta} \tag{4.12}$$

It should be noted that the roundings of corners should be extracted from this value in order to obtain the exact value. Efficiency Q depends on blade width and steel grade. For S355, the efficiency is $Q = 8800$ mm^2/min and for stronger steel grades, $Q = 6900$ mm^2/min.

Finally, the sawing consumables [€/min] are calculated including only the wear of saw blades

$$c_{CS} = \frac{A_t p_{SB}}{S_t T_{PS}} \tag{4.13}$$

where A_t is the total cross-section area of the sawed end [mm^2]. Bevelled ends must

be taken into account in this area so that $A_t = A/\cos\theta$. The price of the saw blade is p_{SB}. Here the price $p_{SB} = 100$ € is used. The durability of the blade S_t [mm^2] is calculated from the formula

$$S_t = Q \cdot F_s \cdot F_{sp} \tag{4.14}$$

where F_s is a parameter that depends on the sawing equipment and F_{sp} is parameter that depends on wall thickness of the cross-section. Here the value $F_s = 1350$ is used for equipment and F_{sp} can be calculated from continuous function as follows:

$$F_{sp} = -1 \cdot 10^{-4} t_{mv}^2 + 0.0159 t_{mv} + 0.3716 \tag{4.15}$$

Finally the total sawing costs of the frame can be calculated by summing the costs of each member. It is important to note that the sawing costs for the member ends may be different because the bevelling angle for both ends may not be same. Therefore costs for member ends must be calculated separately and so Eq. (4.7) is written in form

$$C_{S,i} = c_S T_{NS,i} + \sum_{j=1}^{2} T_{PS,i,j}(c_S + c_{CS,i,j} + c_{EnS}) \tag{4.16}$$

Finally the total sawing costs are computed by

$$C_{\mathrm{S}}(\boldsymbol{x}) = \sum_{i=1}^{n_E} C_{S,i}(\boldsymbol{x}) \tag{4.17}$$

Painting cost

The painting of the structure is done by spray-gun. The roof truss and columns are painted in a separate space. Non-productive time is ignored in calculation because of its minor influence on the total cost. The painting cost is calculated by following equation

$$C_P = T_{PP}(c_{LP} + c_{REP} + c_{SeP})/u_P + c_{CP} \tag{4.18}$$

where T_{PP} is productive painting time, $c_{LP} = 0.46$ [€/min] is unit labour cost,

$c_{REP} = 0.03$ [€/min] is the real estate investment cost, $c_{SeP} = 0.04$ [€/min] is the real estate maintenance cost, $u_P = 1$ is utilization rate and c_{CP} is the cost of painting consumables.

Productive time depends on the chosen painting system. The alkyd painting system is chosen in this thesis. For this painting system, the productive time is

$$T_{PP} = 5.7 \cdot 10^{-7} \cdot A_p \tag{4.19}$$

where A_p is the surface area of the member to be painted. This painting area depends on circumference A_u of the cross-section and member length l. Each member of the frame is painted so the total painting area of the frame is calculated with following equation

$$A_p = \sum_{i=1}^{n_E} A_{u,i} l_i \tag{4.20}$$

The cost of consumables depends on the painting system. As mentioned above, alkyd system is used here. For this painting system the cost of consumables is

$$c_{CP} = 3.87 \cdot 10^{-6} A_p \tag{4.21}$$

Thus, painting cost function can be simplified to the form

$$C_{\mathrm{P}}(\boldsymbol{x}) = 4.1721 \cdot 10^{-6} A_p \tag{4.22}$$

Welding cost

Assembling of the roof truss is done by welding. The roof truss is then connected to columns with bolted plates on construction site. As mentioned previously, only manufacturing costs are considered. This means that only welding of the roof truss is included in the cost function. When non-productive time and equipment maintenance are disregarded, the assembly cost function is expressed in form

$$C_{PA} = T_{PPA}\Big(\frac{c_{LPA} + c_{EqPA} + c_{REPA} + c_{SePA}}{u_{PA}} + c_{EnPA}\Big) + c_{CPA} \tag{4.23}$$

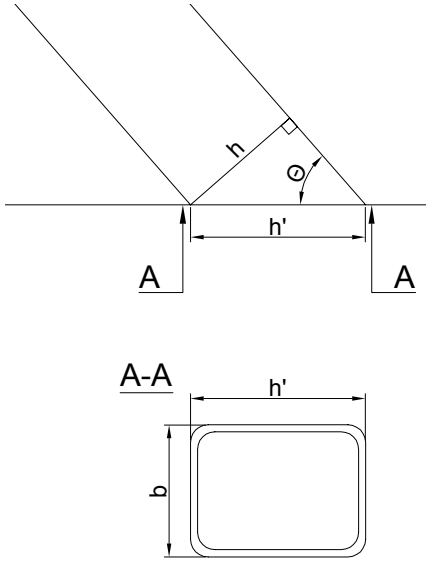

Figure 4.1: *The projected circumference of the welded profile.*

where $c_{LPA} = 0.46$ [€/min] is labour cost, $c_{EqPA} = 0.01$ [€/min] is equipment cost, $c_{REPA} = 0.03$ [€/min] is real estate investment cost, $c_{SePA} = 0.04$ [€/min] is real estate maintenance cost and $c_{EnPA} = 0.01$ [€/min] is energy cost. Utilization rate is set to $u_{PA} = 1$.

Productive time T_{PPA} is comprised of tacking time and welding time

$$T_{PPA} = T_{PTa} + T_{Pw} \tag{4.24}$$

where $T_{PTa} = 1.59$ [min] is the tacking time for one member and T_{Pw} is the welding time. For this thesis, gas metal arc welding with mixed gas (MAG M) was chosen. Thus, the welding time [min] for fillet welds can be calculated with following formula

$$T_{Pw} = (0.4988a^2 - 5 \cdot 10^{-4}a + 2.1 \cdot 10^{-3})\frac{L_{fw}}{1000} \tag{4.25}$$

where L_{fw} is the weld length [mm] and a is the weld size [mm]. The weld length is the circumference of the profile which is projected to the surface where the profile is welded.

The height of the projected cross-section depends on the welding angle θ so that $h' = h/\sin\theta$ (see Fig. 4.1). Thus, the weld length is calculated in the following manner

$$L_{fw} = 2(h' - 2r + b - 2r) + 2\pi r = 2\Big(\frac{h}{\sin\theta} + b\Big) + (2\pi - 8)r \tag{4.26}$$

Usually equal strength fillet welds are used for welded structures. The weld sizes of equal strength fillet welds for different steel grades are presented in [26]. The weld size is $a = 1.11t$ for grade S355 and $a = 1.48t$ for S420. For grade S700 the fillet weld size is $a = 1.65t$.

The cost of welding consumables is c_{CPA} [€]. It includes the costs of welding wire and shield gas. For fillet welds the welding consumable cost can be derived from

$$c_{CPA} = 7.85 \cdot 10^{-6} \cdot 6.35 L_{fw} a^2 \tag{4.27}$$

Finally, the welding cost of a single member can be expressed with formula

$$C_{PA,i} = T_{PTa} c_{PA} + \sum_{j=1}^{2} T_{pw,i,j} c_{PA} + c_{CPA,i,j} \tag{4.28}$$

where $c_{PA} = (c_{LPA} + c_{EqPA} + c_{REPA} + c_{SePA})/u_{PA} + c_{EnPA}$. The welding time is determined separately for both ends j of member i because the welding lengths may vary depending on the angle θ.

Finally, the welding cost of the whole frame is calculated by adding up costs of single members

$$C_{\mathrm{PA}}(\boldsymbol{x}) = \sum_{i=1}^{n_E} C_{PA,i} \tag{4.29}$$

4.3 Constraints

The usability of the portal frame and compliance with the relevant design rules are ensured by the constraints. All the relevant design criteria were presented previously in Section 2.2. There are different ways to formulate constraints. In Eurocode design criteria are presented in following way

$$E_{\mathrm{d}} \leq R_{\mathrm{d}} \tag{4.30}$$

where E_d is the design value of forces or stresses and R_d is the design value of resistance. Design values of forces are calculated at both ends of the member i and the larger value is placed in constraints. In optimization inequality constraints should be presented in the form $g_\mathrm{j}(\boldsymbol{x}) \leq 0$.

Constraint for axial force can be derived from Eqs. (2.5) and (2.6).

$$g_\mathrm{i}^N(\boldsymbol{x}) = \begin{cases} N_{\mathrm{Ed,i}}(\mathbf{x}) - N_{\mathrm{Rd,i}}(\mathbf{x}) \leq 0 \\ -N_{\mathrm{Ed,i}}(\mathbf{x}) - N_{\mathrm{Rd,i}}(\mathbf{x}) \leq 0 \end{cases} \tag{4.31}$$

Axial capacity $N_{\mathrm{Rd,i}}(\mathbf{x})$ of member i is calculated from Eq. (2.7). Here the common sign convention is employed meaning that tension is positive and compression negative. In the case of tension force, the upper part of this equation pair becomes active. Respectively, the lower part becomes active when member is under compression.

Criteria for the bending resistance is written in Eq. (2.8). The effect of axial force (Eq. (2.10)) must be taken into account in bending capacity.

$$g_\mathrm{i}^M(\boldsymbol{x}) = M_{\mathrm{Ed,i}}(\mathbf{x}) - M_{\mathrm{N,Rd,i}}(\mathbf{x}) \leq 0 \tag{4.32}$$

Respectively, constraint for shear resistance is

$$g_\mathrm{i}^V(\boldsymbol{x}) = V_{\mathrm{Ed,i}}(\mathbf{x}) - V_{\mathrm{Rd,i}}(\mathbf{x}) \leq 0 \tag{4.33}$$

Buckling must be checked for members under compression. Both in and out of the plane is considered. Negative value of design axial force is selected so that buckling constraint is active only for the compressed members.

$$g_\mathrm{i}^B(\boldsymbol{x}) = \begin{cases} -N_{\mathrm{Ed,i}}(\mathbf{x}) - N_{\mathrm{b,Rd,y,i}}(\mathbf{x}) \leq 0 & \text{in plane} \\ -N_{\mathrm{Ed,i}}(\mathbf{x}) - N_{\mathrm{b,Rd,z,i}}(\mathbf{x}) \leq 0 & \text{out of plane} \end{cases} \tag{4.34}$$

Constraint for combined compression and bending is respectively

$$g_\mathrm{i}^C(\boldsymbol{x}) = \begin{cases} -\dfrac{N_{\mathrm{Ed,i}}(\mathbf{x})}{N_{\mathrm{b,Rd,y,i}}(\mathbf{x})} + k_{yy}(\mathbf{x})\dfrac{M_{\mathrm{Ed,i}}(\mathbf{x})}{M_{\mathrm{pl,Rd,i}}(\mathbf{x})} - 1 \leq 0 & \text{in plane} \\ -\dfrac{N_{\mathrm{Ed,i}}(\mathbf{x})}{N_{\mathrm{b,Rd,z,i}}(\mathbf{x})} + k_{zy}(\mathbf{x})\dfrac{M_{\mathrm{Ed,i}}(\mathbf{x})}{M_{\mathrm{pl,Rd,i}}(\mathbf{x})} - 1 \leq 0 & \text{out of plane} \end{cases} \tag{4.35}$$

Linear constraint for cross-section classification is written for every member of the frame so that

$$g_{\mathrm{i}}^{CL}(\boldsymbol{x}) = h_i - 2r_i - 38\epsilon t_i \leq 0 \tag{4.36}$$

Constraint for the truss members in welded joints was presented in Eq. (2.23). This constraint can also be expressed in linear form

$$g_{\mathrm{i}}^{G1}(\boldsymbol{x}) = h_i - 35t_i \leq 0 \tag{4.37}$$

where i is a member of the roof truss. The side lengths of braces are limited by the side lengths of chords

$$g_{\mathrm{i}}^{G2}(\boldsymbol{x}) = \begin{cases} h_{bi} - 0.85h_{tc} \leq 0 \\ h_{bi} - 0.85h_{bc} \leq 0 \end{cases} \tag{4.38}$$

$$g_{\mathrm{i}}^{G3}(\boldsymbol{x}) = \begin{cases} 0.35h_{tc} - h_{bi} \leq 0 \\ 0.35h_{bc} - h_{bi} \leq 0 \end{cases} \tag{4.39}$$

where h_{bi} is the side length of the brace i.

Joint resistance constraints for K-, N- and KT-joints are formed based on four possible failure modes. The resistances must be checked at each joint for both brace members. In order to avoid chord face failure of the joint j the normal force in brace $i \in [1, 2]$ is limited by following constraint

$$g_{\mathrm{j}}^{CF}(\boldsymbol{x}) = \begin{cases} N_{\mathrm{Ed,i}}(\mathbf{x}) - \dfrac{8.9 f_{y0} t_0^2 \sqrt{\gamma}\beta}{\sin\theta_i} \leq 0 \\ -N_{\mathrm{Ed,i}}(\mathbf{x}) - \dfrac{8.9 f_{y0} t_0^2 \sqrt{\gamma}\beta}{\sin\theta_i} \leq 0 \\ -N_{\mathrm{Ed,i}}(\mathbf{x}) - \dfrac{8.9 f_{y0} t_0^2 \sqrt{\gamma}}{\sin\theta_i}(1.3\beta - 0.4n) \leq 0 \end{cases} \tag{4.40}$$

The upper part of the equation is active when the brace is under tension. The other two parts of the constraint become active when the brace is compressed.

Furthermore, the constraint for chord shear failure is written in form

$$g_{\mathrm{j}}^{CS}(\boldsymbol{x}) = \begin{cases} N_{\mathrm{Ed,i}}(\mathbf{x}) - \dfrac{f_{y0}A_{v0}}{\sqrt{3}\sin\theta_i} \leq 0 \\ -N_{\mathrm{Ed,i}}(\mathbf{x}) - \dfrac{f_{y0}A_{v0}}{\sqrt{3}\sin\theta_i} \leq 0 \\ N_{Ed,0}(\mathbf{x}) - \Big((A_0 - A_v)f_{\mathrm{y}0} + A_v f_{\mathrm{y}0}\sqrt{1-(V_{\mathrm{Ed}}/V_{\mathrm{pl,Rd}})^2}\Big) \leq 0 \\ -N_{Ed,0}(\mathbf{x}) - \Big((A_0 - A_v)f_{\mathrm{y}0} + A_v f_{\mathrm{y}0}\sqrt{1-(V_{\mathrm{Ed}}/V_{\mathrm{pl,Rd}})^2}\Big) \leq 0 \end{cases} \tag{4.41}$$

where $N_{Ed,0}$ is the design axial force of the chord. The brace failure constraint is

$$g_{\mathrm{j}}^{BF}(\boldsymbol{x}) = \begin{cases} N_{\mathrm{Ed,i}}(\mathbf{x}) - f_{\mathrm{yi}}t_{\mathrm{i}}(2h_{\mathrm{i}} - 4t_{\mathrm{i}} + b_{\mathrm{i}} + b_{eff}) \leq 0 \\ -N_{\mathrm{Ed,i}}(\mathbf{x}) - f_{\mathrm{yi}}t_{\mathrm{i}}(2h_{\mathrm{i}} - 4t_{\mathrm{i}} + b_{\mathrm{i}} + b_{eff}) \leq 0 \end{cases} \tag{4.42}$$

The fourth possible failure mode for KT-joints is punching shear failure which is expressed as

$$g_{\mathrm{j}}^{PS}(\boldsymbol{x}) = \begin{cases} N_{\mathrm{Ed,i}}(\mathbf{x}) - \dfrac{f_{\mathrm{y}0}t_0}{\sqrt{3}\sin\theta_{\mathrm{i}}}\Big(\dfrac{2h_{\mathrm{i}}}{\sin\theta_{\mathrm{i}}} + b_{\mathrm{i}} + b_{\mathrm{e,p}}\Big) \leq 0 \\ -N_{\mathrm{Ed,i}}(\mathbf{x}) - \dfrac{f_{\mathrm{y}0}t_0}{\sqrt{3}\sin\theta_{\mathrm{i}}}\Big(\dfrac{2h_{\mathrm{i}}}{\sin\theta_{\mathrm{i}}} + b_{\mathrm{i}} + b_{\mathrm{e,p}}\Big) \leq 0 \end{cases} \tag{4.43}$$

In the case of Y-joint only chord face failure is considered. This constraint can be formed by same principle as the chord face failure of K/N-joint. The common sign convention is once again employed so that

$$g_{\mathrm{j}}^{CF}(\boldsymbol{x}) = \begin{cases} N_{\mathrm{Ed}}(\mathbf{x}) - \dfrac{f_{y0}t_0^2}{(1-\beta)\sin\theta}\Big(\dfrac{2\eta}{\sin\theta} + 4\sqrt{1-\beta}\Big) \leq 0 \\ -N_{\mathrm{Ed}}(\mathbf{x}) - \dfrac{f_{y0}t_0^2}{(1-\beta)\sin\theta}\Big(\dfrac{2\eta}{\sin\theta} + 4\sqrt{1-\beta}\Big) \leq 0 \\ -N_{\mathrm{Ed}}(\mathbf{x}) - \dfrac{(1.3-0.4n/\beta)f_{y0}t_0^2}{(1-\beta)\sin\theta}\Big(\dfrac{2\eta}{\sin\theta} + 4\sqrt{1-\beta}\Big) \leq 0 \end{cases} \tag{4.44}$$

Finally all the joint resistance constraints are gathered into one constraint

$$g_{\mathrm{j}}^{J}(\boldsymbol{x}) = \{g_{\mathrm{j}}^{CF}(\boldsymbol{x})\, g_{\mathrm{j}}^{CS}(\boldsymbol{x})\, g_{\mathrm{j}}^{BF}(\boldsymbol{x})\, g_{\mathrm{j}}^{PS}(\boldsymbol{x})\} \tag{4.45}$$

In addition to joint resistance constraints also gap constraints are included to problem so that joint resistances are valid. The following constraint is checked for K-, N- and KT-joints.

$$g_{\mathrm{j}}^{Gap}(\boldsymbol{x}) = \begin{cases} t_1 + t_2 - g \leq 0 \\ 0.5b_0(1-\beta) - g \leq 0 \\ g - 1.5b_0(1-\beta) \leq 0 \end{cases} \tag{4.46}$$

4.4 Formulation of the problem

Optimization problem of the single portal frame in standard form is

$$\begin{aligned} &\min f(\boldsymbol{x}) \\ &\text{subject to} \\ &\quad g_{\mathrm{i}}^{N}(\boldsymbol{x}) \leq 0 \qquad i = 1, 2..., n_{\mathrm{E}} \\ &\quad g_{\mathrm{i}}^{M}(\boldsymbol{x}) \leq 0 \qquad i = 1, 2..., n_{\mathrm{E}} \\ &\quad g_{\mathrm{i}}^{V}(\boldsymbol{x}) \leq 0 \qquad i = 1, 2..., n_{\mathrm{E}} \\ &\quad g_{\mathrm{i}}^{B}(\boldsymbol{x}) \leq 0 \qquad i = 1, 2..., n_{\mathrm{E}} \\ &\quad g_{\mathrm{i}}^{C}(\boldsymbol{x}) \leq 0 \qquad i = 1, 2..., n_{\mathrm{E}} \\ &\quad g_{\mathrm{i}}^{CL}(\boldsymbol{x}) \leq 0 \qquad i = 1, 2..., n_{\mathrm{E}} \\ &\quad g_{\mathrm{i}}^{G1}(\boldsymbol{x}) \leq 0 \qquad i = 1, 2..., n_{\mathrm{E,t}} \\ &\quad g_{\mathrm{i}}^{G2}(\boldsymbol{x}) \leq 0 \qquad i = 1, 2..., n_{B} \\ &\quad g_{\mathrm{i}}^{G3}(\boldsymbol{x}) \leq 0 \qquad i = 1, 2..., n_{B} \\ &\quad g_{\mathrm{j}}^{J}(\boldsymbol{x}) \leq 0 \qquad j = 1, 2..., n_{J} \\ &\quad g_{\mathrm{j}}^{Gap}(\boldsymbol{x}) \leq 0 \qquad j = 1, 2..., n_{J} \end{aligned} \tag{4.47}$$

where $f(\boldsymbol{x})$ is the objective function (mass or cost). n_{E} is a total number of members in the frame, $n_{\mathrm{E,t}}$ is a number of truss members, n_B is a number of braces and n_J is a number of joints excluding chord-to-columns and column-base connections. Welded joint geometry constraints are applied only to truss members. $\mathbf{x}$ is the vector containing all the variables. When braces are considered to be same, there are only $n_{\mathrm{var}} = 8$ variables. When braces are optimized in symmetry pairs, the number of variables is $n_{\mathrm{var}} = 2n_{\mathrm{sym}}$, where n_{sym} is the number of symmetry pairs.

5. CALCULATION EXAMPLES

Optimization of a trussed steel portal frame is studied with seven different test cases. All the cases are calculated on a computer with Intel Core i7-3770 processor, running 3.4 GHz clock frequency with 16 GB RAM. The benchmark structure is a portal frame with geometry and loads according to Fig. 5.1.

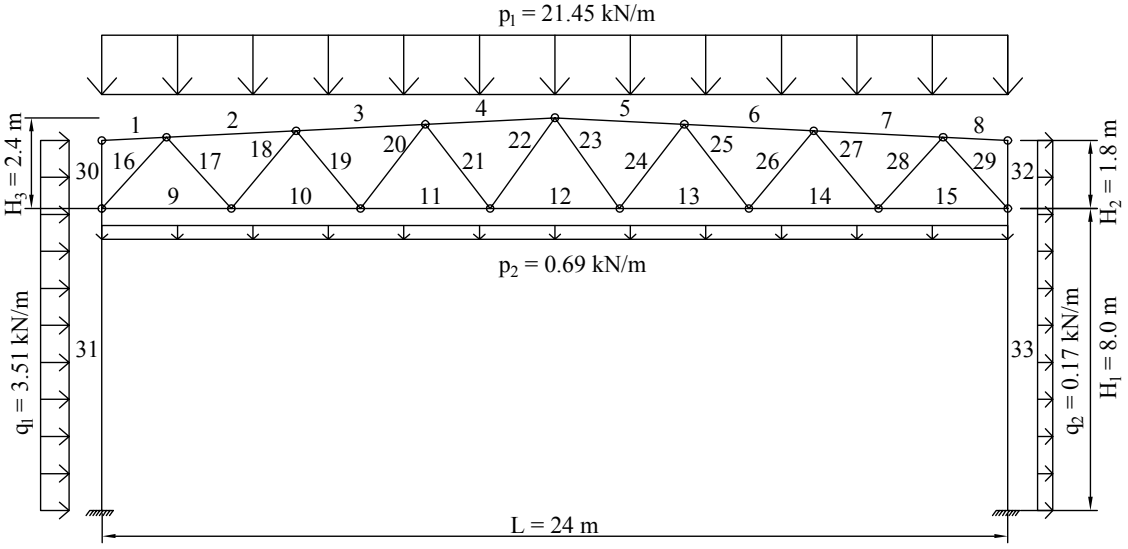

Figure 5.1: *The benchmark case.*

Dimensions in the figure are measured from mid-lines of members. The span of the roof truss is $L = 24$ m and heights of the columns are $H_1 + H_2 = 8.0 + 1.8 = 9.8$ m. The height of the truss in the middle of span is $H_3 = 2.4$ m. The line load of top chord is $p_1 = 21.45$ kN/m which includes typical snow load in southern Finland and the dead load of roof structures. The hanging load of bottom chord is $p_2 = 0.69$ kN/m. Wind loads are $q_1 = 3.51$ kN/m for windward column and $q_2 = 0.17$ kN/m for leeward column. All the loads are combined according to Eurocode [9] with snow load being the leading variable action.

The other six test cases are created by changing the span of the truss L, loads p_1, q_1 and q_2 or the truss topology. Cases 2 and 3 are frames that are similar to the benchmark frame with respect to geometry and truss topology. Case 2 is a frame that

Table 5.1: *The test cases.*

Case	**L [m]**	**Truss [-]**	p_1 **[kN/m]**	q_1 **[kN/m]**	q_2 **[kN/m]**
1	24	K	21.45	3.51	0.17
2	24	K	30.45	3.51	0.17
3	24	K	16.05	5.85	0.28
4	20	K	21.45	3.51	0.17
5	30	K	21.45	3.51	0.17
6	24	KT	21.45	3.51	0.17
7	24	N	21.45	3.51	0.17

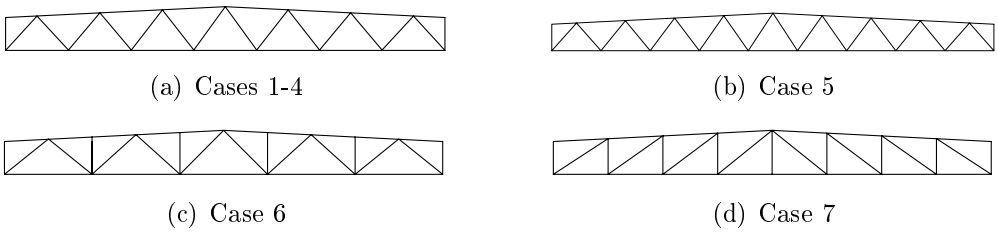

(a) Cases 1-4 (b) Case 5

(c) Case 6 (d) Case 7

Figure 5.2: *Layout of trusses.*

has larger top chord load. In the case 3, wind load is considered being the leading variable action making the horizontal loads larger and top chord load smaller.

Cases 4 and 5 are frames in which only the span of the truss varies (20 m and 30 m). They are considered similar to the benchmark frame with respect to loading conditions. Cases 6 and 7 are same as the benchmark in respect of both span and loads. Case 6 is a KT-trussed frame and case 7 is a N-trussed frame. The same steel grades are used for every test case. Chords are S420 grade and columns and braces are S355 grade. Table 5.1 summarizes how the span, truss topology and loads vary between test cases. Heights H_1 and H_2, the roof slope s and bottom chord load p_2 remain same in every case.

Fig. 5.2 illustrates topologies of test cases. Cases 1-4 have identical truss topology with K-truss. Case 5 has also K-truss, but the number and division of the braces are different due to the longer span. Division of braces in KT-truss is rather sparse so that joint eccentricities can be minimized in KT-joints. With denser division, it becomes difficult to meet the gap and geometry requirements of the joints. In N-truss braces are modeled so that the outermost braces are connected to the joint between column and bottom chord.

5.1 Mass optimization

The mass optimization of the frames is studied both with and without joint resistance constraints. Due to stochastic nature of Genetic Algorithm, each test case was optimized 10 times first without joint constraints and then again 10 times with joints. The purpose was to study how much joint constraints affect the minimum-mass solution, the standard deviation of the solutions and the calculation time. The results were studied by statistical quantities to see the variation of the solutions. Table 5.2 shows results of these 10 optimization runs for each test case. The results include the best and mean result. Also standard deviation (std) is calculated to see how much the results vary and the mean calculation time is presented as well.

Table 5.2: *The mass optimization results.*

	Mass without joints				**Mass with joints**			
Case	**Best [kg]**	**Mean [kg]**	**Std [%]**	**Mean time [min]**	**Best [kg]**	**Mean [kg]**	**Std [%]**	**Mean time [min]**
1	2258	2326	1.1	11	2346	2397	1.5	12
2	2804	2854	1.3	12	2967	3056	2.3	15
3	2091	2114	0.9	10	2192	2209	0.6	12
4	1798	1824	1.8	11	1890	1926	1.3	14
5	3248	3310	1.8	15	3453	3559	2.3	19
6	2163	2223	1.1	10	2255	2346	3.1	11
7	2298	2372	1.9	11	2480	2543	2.6	12

The standard deviations indicate that variation of the solutions is relatively small and within acceptable limits. Including joints in constraints does not seem to have a major impact on the variation. For some test cases the standard deviation even decreased when joint constraints were added. The statistics indicate that the four-stage procedure can produce solutions within a small range of variation.

When comparing the results of test cases with/without joints, it is noteworthy that including joints in constraints increases the mass of the frames by 4-8% depending on the geometry and loads of the test case. Joint constraints influence most on the case 5 (6.3%) and case 7 (7.9%).

The mean time of the optimization process was also observed because reasonable calculation time was one of the main criteria for the optimization method. The mean time ranged from 11 to 19 minutes when joint constraints were introduced. Case 5 was clearly the most time-consuming test case. The optimization time remained within 11 to 15 minutes for other test cases while the optimization time of the case 5 was approximately 19 minutes. The reason for this is the longer span (30 m)

Table 5.3: *The relative masses of optimum solutions.*

Case	Total mass [kg]	Relative mass [-]
1	2346	1.00
2	2967	1.26
3	2192	0.93
4	1890	0.80
5	3453	1.47
6	2255	0.96
7	2480	1.06

and therefore the larger number of elements in the FE-model. While the number of members is large the time involved in one function evaluation grows.

Table 5.3 presents comparison between test cases. The relative mass of each test case has been calculated with relation to the benchmark case 1 when all the relevant Eurocode 3 design rules are considered.

Table 5.3 illustrates that increasing the horizontal top chord load by 40% (case 2) causes the total mass grow by 26%. In case 3, the mass of the frame decreases by 7% when top chord load is reduced and wind loads are increased. Changing of the span has also impact on the total mass. Reducing the benchmark span by 17% leads to 20% lighter structure. Respectively, increasing the span of the benchmark frame by 25% results in almost 50% heavier structure.

When comparing different topologies (cases 6-7), it is noticed that KT-frame gives the lightest structure with given loads and geometry. KT-frame reaches 4% lighter structure than benchmark case with K-truss. N-trussed frame is the heaviest solution of these three topologies with relative mass being 6% bigger compared to the benchmark case.

5.1.1 Optimum profiles

The optimum profiles are presented in Table 5.4 for each test case when joints are included in constraints. Also the highest utilization rate concerning member strength and buckling is calculated. In the table only the most stressed brace member is presented for simplification since the test cases have different number of braces depending on the span and topology of the truss. The most stressed brace is the outermost brace of the truss in each test case.

Table 5.4 indicates that high utilization rates are achieved for columns in every test

Table 5.4: *The optimum profiles of each test case when all the constraints are considered. Highest utilization rate of member strength and buckling is presented in brackets.*

Case	Columns	Top chord	Bottom chord	Outermost brace
1	220x7.1 (98%)	160x6 (85%)	120x6 (83%)	100x4 (91%)
2	250x7.1 (95%)	160x8 (96%)	150x7.1 (80%)	120x4 (93%)
3	220x8 (94%)	150x5 (86%)	110x5 (83%)	90x4 (79%)
4	220x7.1 (82%)	140x5 (84%)	120x5 (79%)	100x3 (86%)
5	250x8 (93%)	180x6 (95%)	150x7.1 (72%)	120x4 (83%)
6	220x7.1 (99%)	140x5 (100%)	140x6 (66%)	110x4 (91%)
7	220x7.1 (90%)	150x5 (75%)	150x6 (54%)	120x5 (83%)

case. High utilities are also attained for the outermost brace members. Utility of top chord is also relatively high with the exception of case 7. The reason for this is the heavily loaded N-joint where the constraint of chord face failure is active. This joint is the outermost N-joint of top chord where the most compressed diagonal is connected to the chord. This joint limits the top chord profile so that utilization of member strength and buckling stays low.

The utilities of bottom chord are smaller compared to top chord in each test case. This is also due to the joint resistances. Especially in the cases 6 and 7 the chord face failure of Y-joint is the active constraint for bottom chord. This Y-joint is located at the bottom corner of truss where the most compressed brace member is connected to the bottom chord. As a result, utility of member strength remains low in bottom chord. This is likely to be due to the placement of brace members in KT- and N-trusses. The forces in joints between bottom chord and braces could have possibly been reduced with different placement of braces in which case the more reasonable bottom chord profile may have been obtained.

In above-mentioned situations the reinforcement of the most heavily loaded joints should be considered. When chord profiles are decided by only few joints it may be reasonable to reinforce the most critical joints instead of choosing larger chord profiles.

5.1.2 Mass distribution

Optimum solutions can also be used to calculate the distribution of mass. Masses of columns, chords and braces are calculated separately to see which structural components affect the most on the total mass of the frame. Table 5.5 represents the mass distribution of optimum solutions by the structural components.

Table 5.5: *The mass distribution.*

Case	Columns [kg]	Top chord [kg]	Bottom chord [kg]	Braces [kg]
1	904 (39%)	680 (29%)	498 (21%)	264 (11%)
2	1035 (35%)	876 (30%)	732 (25%)	324 (11%)
3	1010 (46%)	535 (24%)	384 (18%)	264 (12%)
4	904 (48%)	414 (22%)	351 (19%)	221 (12%)
5	1158 (34%)	963 (28%)	915 (26%)	417 (12%)
6	904 (40%)	497 (22%)	588 (26%)	266 (12%)
7	904 (36%)	535 (22%)	634 (26%)	408 (16%)

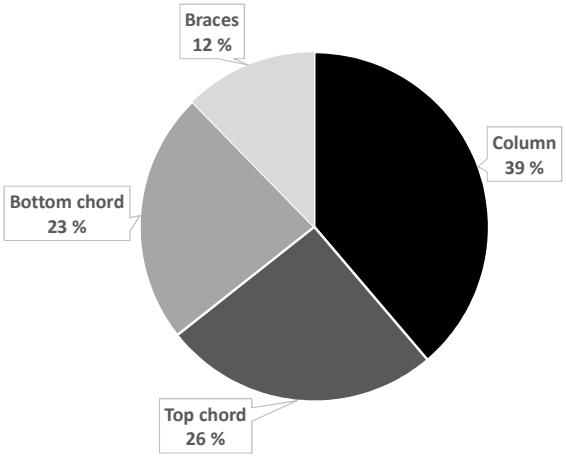

Figure 5.3: *The average mass distribution of the frame.*

The results in Table 5.5 suggest that most of the material consumption of the frame comes from columns. Columns compose the largest part of the total mass in every test case. Their proportion varies between 34-48% of the total mass. Top chord composes the next largest part in cases 1-5. Cases 6-7 gave larger bottom chord profile which naturally led to larger mass than top chord.

Braces form relatively small part of the total mass. Their proportion is 11-12% in cases 1-6. N-trussed test case is the only case where the proportion of braces is larger (16%). This is probably due to the choice of placement of the braces. The long diagonals of the N-truss (see Fig. 5.2) are compressed and short verticals are tensioned in the optimum solution. This results in rather big profiles for diagonals as shown in Table 5.4. Changing the positioning of the braces in such way that the outermost diagonals would be connected to the top chord instead of bottom chord could lead to smaller brace profiles. This could reduce the proportion of the total mass that is comprised of brace members.

The average distribution of total mass of the portal frame is calculated based on the

results presented in Table 5.5. Fig. 5.3 illustrates how the total mass is distributed in the frame by the structural components.

5.2 Cost optimization

The cost functions that were presented in subsection 4.2.2 are employed in cost optimization. Employment of functions is fairly straightforward for the material, blasting and painting costs. Sawing and welding has to be determined separately for every frame member.

Sawing and welding costs are simple to determine for braces, because every brace is modeled with one member in structural model. Thus, sawing and welding costs can be calculated in both ends for every brace member. This principle can not be used for chords and columns because they are modeled with more than one member in the structural model. Top chord is manufactured in two pieces so totally four ends need to be sawed. The pieces are welded together which is taken into account in the welding function. Bottom chord is manufactured as one piece in which case two ends are sawed and welded. In the case of columns welding is ignored and only sawing for both ends is included.

The cost optimization was carried out with the same principle as the mass optimization. Each of the seven test cases was again optimized 10 times both with and without joint resistance constraints. Table 5.6 summarizes the statistics of these optimization runs for each test case.

Table 5.6: *The cost optimization results.*

	Cost without joints				**Cost with joints**			
Case	**Best [€]**	**Mean [€]**	**Std [%]**	**Mean time [min]**	**Best [€]**	**Mean [€]**	**Std [%]**	**Mean time [min]**
1	2407	2464	2.3	10	2504	2552	1.3	11
2	2943	2984	1.0	12	3097	3126	0.7	15
3	2262	2301	1.3	10	2332	2371	1.0	12
4	1964	2017	2.2	8	2046	2076	1.0	13
5	3457	3489	1.1	17	3616	3699	1.7	19
6	2344	2377	2.1	10	2442	2480	1.9	12
7	2629	2681	1.9	13	2730	2791	1.2	14

The table illustrates that the standard deviation of results remain low as in the mass optimization. Introducing the joint constraints has still no negative effect on variability of results. On the contrary, standard deviation decreases slightly after

adding joint constraints with the exception of case 5. The standard deviation remains under 2% for every test case when joints are introduced.

The relative change in the cost when the joint resistances are added into constraints does not vary significantly between test cases. The joint constraints increase the total cost by 3-5%. The smallest change happens in case 3 (3.1%) where vertical loads are larger. The highest growth in the cost occurs for the case 2 (5.2%) with larger top chord load.

The mean time for cost optimization remained the same as for mass optimization. The mean time ranged from 11 to 19 minutes between test cases when joints were considered in the problem. Case 5 with the longest span was again clearly the most time-consuming case with calculation time of 19 minutes. Cost optimization of all the other test cases took 11-15 minutes.

5.2.1 Optimum profiles

The profiles of cost optimums are illustrated in Table 5.7. In the table only the largest brace profile is presented for simplification.

Table 5.7: *The profiles of cost optimums.*

Case	Columns	Top chord	Bottom chord	Outermost brace	Total cost [€]
1	220x7.1	160x6	120x6	100x4	2504
2	250x7.1	160x8	150x7.1	120x4	3097
3	220x8	150x5	110x5	90x4	2332
4	220x7.1	140x5	120x5	100x3	2046
5	250x8	180x6	150x7.1	120x4	3616
6	220x7.1	140x5	140x6	110x4	2442
7	220x7.1	150x5	150x6	120x5	2730

Comparison between the cost optimums and the mass optimums presented in Table 5.4 points out that there is no difference between mass and cost optimum. The identical result was obtained with both mass and cost optimization in every test case. In addition to the outermost braces, also all the other braces got the same profile in both cost and mass optimum.

From this it can be concluded that the mass can be chosen as the objective function instead of costs with the cost functions and parameters applied in this thesis. This choice leads not only to mass optimum but also to cost optimum or at least very close to it. It should be acknowledged that the cost optimum depends on the chosen functions and parameters.

5.2.2 The break-down of costs

The total cost can be broken down to separate cost components to see which components have the most impact on the total cost of the frame. Table 5.8 presents a breakdown of the costs for each test case when joints are considered in optimization.

Table 5.8: *The breakdown of total costs of the whole frame.*

Case	Material [€]	Blasting [€]	Sawing [€]	Welding [€]	Painting [€]	Total [€]
1	1947 (78%)	38 (2%)	206 (8%)	91 (4%)	222 (9%)	2504
2	2469 (79%)	38 (1%)	213 (7%)	132 (4%)	244 (8%)	3097
3	1800 (77%)	38 (2%)	204 (9%)	78 (3%)	212 (9%)	2332
4	1548 (76%)	34 (1%)	202 (9%)	70 (3%)	192 (8%)	2046
5	2875 (80%)	47 (1%)	260 (7%)	131 (4%)	303 (8%)	3616
6	1877 (77%)	39 (2%)	204 (8%)	99 (4%)	222 (9%)	2442
7	2060 (75%)	41 (2%)	228 (8%)	156 (6%)	245 (9%)	2730

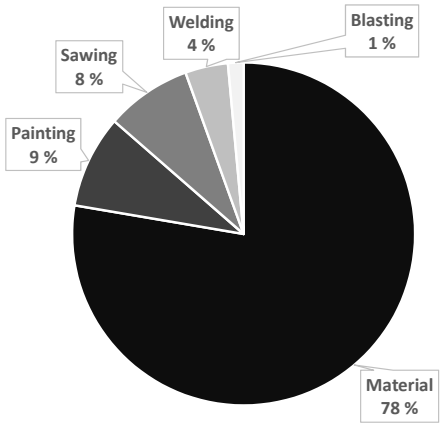

Figure 5.4: *The average cost distribution of the frame.*

The table illustrates that material cost is the major part of total costs. It composes 75-80% of total costs. This outcome explains why the cost optimization results are exactly the same as mass optimization results. With material cost being clearly the largest part of total costs, it is natural that cost minimization leads to nearly identical or even identical solution as mass minimization.

Painting and sawing are the next largest cost components. They constitute together almost 20% of total costs. Welding and blasting have only little significance to the total cost. Only for N-trussed frame the welding costs are rather high. This comes from large profiles of diagonals which increases welding costs of braces. Fig. 5.4 presents the average cost distribution of the trussed portal frame calculated from these seven test cases.

Table 5.9: *The cost distribution by structural components.*

Case	Columns [€]	Top chord [€]	Bottom chord [€]	Braces [€]
1	826 (33%)	716 (29%)	493 (20%)	469 (19%)
2	943 (30%)	907 (30%)	707 (23%)	540 (17%)
3	911 (39%)	576 (25%)	391 (17%)	454 (19%)
4	826 (40%)	455 (22%)	358 (17%)	407 (20%)
5	1042 (29%)	993 (27%)	881 (24%)	701 (19%)
6	826 (34%)	537 (22%)	580 (24%)	499 (20%)
7	826 (30%)	576 (21%)	623 (23%)	705 (26%)

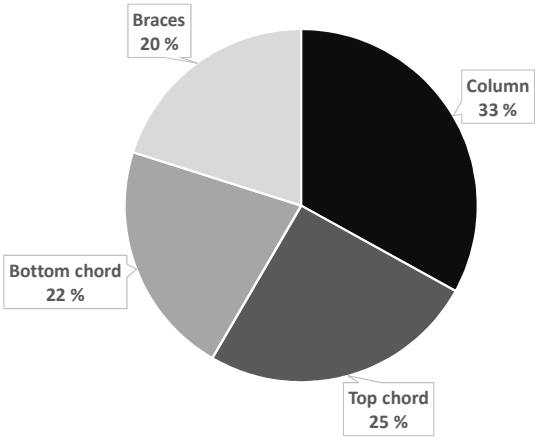

Figure 5.5: *The average cost distribution between structural components.*

In addition to the cost components, total cost can also be calculated for structural components. In Table 5.9 costs are calculated for columns, chords and braces separately.

Table 5.9 shows that cost distribution varies significantly between test cases. Columns are the most expensive structural components in every test case and they constitute 30-40% of total costs. Top chord composes the next largest part of costs in K-trussed test cases (1-5) with proportion being between 22% and 30%. The largest proportion of top chord is achieved with big top chord load and long span. In the case of KT- and N-truss the proportion of top chord is lower.

The proportion of bottom chord and braces are roughly same size in K-trussed test cases. The largest proportion of bottom chord is achieved with bigger top chord load (23%) and longer span (24%). With smaller top chord load and shorter span the proportion of bottom chord reduces down to 17%. The proportion of braces varies between 17% and 20% in K-trussed frames.

In KT-trussed frame bottom chord constitutes the second largest part of total costs.

This results from larger bottom chord profile which increases material cost of the bottom chord. In N-trussed frame braces are the second most expensive structural component. This is a result of large profiles of diagonals which increases welding costs as shown previously in Table 5.8. The costs presented in Table 5.9 can be used to calculate the average cost distribution among structural components. Fig. 5.5 illustrates this average distribution between structural components.

5.3 High-strength steels

Previously optimized test cases included only the most common steel grades S355 and S420. Now high-strength steels (HSS) are introduced to the optimization so that chords are S700 grade and columns and braces are S420. This hybrid HSS-frame is optimized with same geometry and loads as the benchmark frame 1 to compare how the results change. The mass is chosen as objective function and total cost is calculated for the mass optimum. Constraints include all the relevant Eurocode 3 demands. Table 5.10 shows the comparison between the HSS-frame and the frame with regular strength steels. Brace numbering follows the same numbering as shown in Fig. 5.1 with members 16 and 29 being the outermost braces and members 22 and 23 being the pair in the middle of the span.

Table 5.10: *The comparison between the benchmark frame and the HSS-frame.*

	Mass optimum	
	Case 1	**HSS**
Columns	220x7.1	220x7.1
Top Chord	160x6	140x6
Bottom Chord	120x6	100x5
Braces 16 & 29	100x4	80x5
Braces 17 & 28	70x3	50x4
Braces 18 & 27	90x3	80x4
Braces 19 & 26	60x4	60x3
Braces 20 & 25	70x3	70x3
Braces 21 & 24	60x3	50x3
Braces 22 & 23	60x3	50x3
Mass [kg]	2346	2084
Relative mass	1.00	0.89
Cost [€]	2504	2532
Relative cost	1.00	1.01

Table 5.10 illustrates that the use of high-strength steels in profiles gives both material and cost savings. The hybrid S700/S420 frame is 11% lighter than the conventional S420/S355 frame. The results indicate that the greatest material savings are

gained for chords. The smaller material consumption is also achieved for brace members. In the case of columns there is no difference in material consumption despite the stronger steel grade.

In terms of cost, the conventional frame provides a slightly cheaper solution. The high-strength frame is 1% more expensive than the regular-strength frame. This may be due to the material cost factor 1.3 which was used for steel grade S700. Material is spared 11% which apparently is not enough when the material costs of chords are multiplied with the cost factor. With smaller cost factor total costs of high-strength frame could be reduced. If the cost factor for S700 is set to 1.25 according to [29], total cost of hybrid HSS-frame reduces down to 2494 € making it slightly cheaper option than regular-strength frame. Nevertheless, the cost difference is fairly small. In HSS-frame also welding costs are a bit higher because of the larger weld sizes.

Conclusion can be drawn from these results that the use of high-strength steels in the frame gives substantially lighter structure. However, the cost difference is not significant between regular-strength steel frames and HSS-frames. The price of the high-strength steel should be discussed in more detail with the manufacturer in order to get better picture of total costs.

5.4 Calculation time

In the previous optimization results, a maximum number of function evaluations was limited down to 500 in the continuous problem. In the discrete problem time limit was set to 60 seconds. These settings were chosen so that calculation time of the whole optimization problem would not have grown too long. Now these time restrictions are moderated so that the limit of maximum number of function evaluations is set to default value of 3000 in MATLAB. The time limit of Genetic Algorithm is removed entirely. Time limit is replaced by the stopping criterion where the algorithm is stopped if the result has not been improved in last 10 generations.

Optimization results are studied with these new loose time settings to see how much improvement is achieved in optimum solution when the algorithms have more time to search the design space. Here only the benchmark test case 1 is taken under study. The mass of the frame is chosen as objective function. The constraints include also the joint constraints. Table 5.11 presents the comparison between optimum solutions obtained with these new loose time settings and with the previous stricter settings.

The results show that increasing the maximum number of function evaluations in the continuous problem and loosening of the time limit in the discrete problem do

Table 5.11: *The effects of loosening the time restrictions.*

	Stricter time settings	**More loose time settings**
Columns	220x7.1	220x7.1
Top Chord	160x6	160x6
Bottom Chord	120x6	120x6
Braces 16 & 29	100x4	100x4
Braces 17 & 28	70x3	70x3
Braces 18 & 27	90x3	90x3
Braces 19 & 26	60x4	60x3
Braces 20 & 25	70x3	70x3
Braces 21 & 24	60x3	60x3
Braces 22 & 23	60x3	60x3
Mass [kg]	2346	2337
Cost [€]	2504	2494
Calculation time [min]	12	25

not improve the optimum solution almost at all. Smaller profile is found only for the braces 19 and 26. Otherwise the solutions are identical. The improvement in total mass and cost of the frame is under 1% which is nearly non-existent difference.

On the other hand, it should be noted that the best solution out of 10 optimization runs was chosen as a reference solution for the optimization problem where stricter time settings are employed. The mean results of these 10 optimization runs were previously calculated in the Tables 5.2 and 5.6. The mean results 2397 kg and 2552 € were obtained for mass and cost in the benchmark case. By loosening time restrictions the improvement gained in mass and cost are 2-3% as compared to the mean results. This is still a fairly small improvement considering the calculation time that approximately doubles from 12 to 25 minutes when time restrictions are loosened.

Based on these observations it can be assumed that setting time restrictions on the optimization problem is justified. Increasing the calculation time does not provide significant benefits in this optimization method.

5.5 Random starting points

The starting point selection method developed in this thesis is based on the loads and the geometry of the frame. In this section the random starting points are employed in the optimization to study how big influence starting points have on the optimum solution. The benchmark case 1 is taken under study here. 10 random starting points

Table 5.12: *The optimization results of benchmark case when random starting points are employed.*

Optimization run	Mass [kg]	Failing rate [%]
1	2441	50
2	2435	50
3	3093	70
4	2432	50
5	2394	50
6	2355	40
7	2355	50
8	2580	50
9	2454	50
10	2355	50
Best	2355	40
Mean	2489	51

are given manually as starting points for the fmincon-solver in MATLAB. Starting points are generated randomly between the lower and upper bounds of the problem.

In order to obtain comparable results, the optimization is performed 10 times with random starting points. The objective function is mass and constraints include the joint resistances. This way the comparison can be made between random starting points and selection method developed in this thesis. Table 5.12 shows the results of these 10 optimization runs. In the table the mass of the frame and the failing rate of continuous problem are presented. The failing rate of continuous problem describes how many times fmincon-solver fails to find a feasible solution for the given starting points.

The table illustrates that best optimum solution 2355 kg is extremely close to the best solution found with the selection method (2346 kg). Therefore approximately the same optimum solution is achieved with 10 optimization runs regardless of the starting points. However, starting points are relevant regarding the average solution that is attained. The mean result with random starting points is 2489 kg while the mean result with precise selection method was 2397 kg. In other words, random points produce 4% heavier solution in average. Also the standard deviation is 9% for the random points which is noticeably larger deviation than previously. The standard deviation was only 1.5% in the benchmark case when the selection method was used for starting points.

The larger standard deviation is explained by the fact that interior-point algorithm always ends up in the same solution if same starting points are used. Thus, the variability of the final optimum solution is formed only by the stochastic nature of

the Genetic Algorithm if same points are employed. When the points are chosen randomly in each optimization run also the solution of the continuous problem may change.

Table 5.12 shows that average failure rate of continuous problem is 50% meaning that fmincon-solver fails to find a feasible solution for 5 points out of 10 in the continuous stage. With the points chosen by the selection method the failure rate was only 20%. This means that random selection produces more infeasible starting points for the continuous problem than the selection method employed in this thesis.

5.6 Brace optimization

The optimization method developed in this study involves two different problems which both need to be solved in order to obtain the final optimum solution. In the first problem column and chord profiles were optimized. The second problem concerned brace optimization with fixed column and chord profiles. It is reasonable to study how much improvement is made in the optimum solution when the second problem is solved and braces are allowed to have different profiles.

Another noteworthy matter is how much the result is improved during the optimization compared to the best starting point. This point is the starting point that returned lowest objective function value while satisfying the constraints. Starting point selection method developed in this study ignores the profile catalog so the profiles of starting points may not be available in the catalog. The profile catalog was employed after the continuous problem to create the discrete neighborhood.

The brace optimization is studied only with the benchmark case. The results are displayed in Table 5.13. The results include profiles and objective function values for the best starting point and optimum solutions of the first and second problem.

Table 5.13: *The progress of optimum solution during the optimization process.*

	The best starting point	**Only one profile for braces**	**Symmetry pairs**
Columns	230x8	220x7.1	220x7.1
Top Chord	150x6	160x6	160x6
Bottom Chord	127.5x5.1	120x6	120x6
Braces	108.4x4.3	100x4	100x4*
Mass [kg]	2676	2528	2346
Cost [€]	2876	2727	2504

* Only the largest profile is presented here.

The table illustrates that a notable improvement is made in objective function during the optimization. After solving the first problem with one brace profile the mass and cost is reduced by 5-6% compared to the best feasible starting point. At the end of the optimization, a 12% lighter structure is achieved in comparison to the best starting point. In terms of cost the difference is the same magnitude (13%). The changes in profiles show that top chord profile is increased during optimization. Also cross-sectional area of bottom chord becomes larger. On the other hand, the column and brace profiles are decreased which affect the internal forces of the frame so that cross-sections of chords must be enlarged.

The table shows that mass can be reduced by 7% when the symmetry of truss is exploited in brace optimization. In cost optimization symmetrical design offers 8% more cost-effective solution. In a hall building with 10 these kind of portal frames as load-bearing structure, it would mean cost savings worth of over 2000 € which is a considerable saving. These results prove that it is justified to optimize braces more closely to achieve more cost-effective and lighter structure.

6. CONCLUSIONS

The purpose of this study was to develop a procedure for sizing optimization of a trussed steel portal frame that meets all the design criteria for strength and stability presented in Eurocode 3. The main purpose was to discover a procedure that is able to find a feasible solution of high quality to the problem within a reasonable calculation time. The idea was not to devise a procedure that would reach the exact global optimum at the expense of the calculation time.

Both mass and cost minimization were considered in this study. The cross-sectional dimensions of profiles were chosen as variables of the problem. The construction of the FE-model and optimization itself were both implemented in MATLAB.

A four-stage procedure was eventually developed for the problem. This procedure includes two subproblems which both are solved first with continuous variables and then with discrete variables. The idea of relaxing the problems into continuous was to narrow the design space of the discrete problem. In the first subproblem chord and column profiles were optimized. In the latter subproblem brace profiles were optimized with fixed chord and column profiles. The same algorithms were used for both subproblems. The continuous problems were solved by interior-point algorithm for which a separate starting point selection method was developed. Genetic Algorithm was chosen for discrete problems for which the design space was determined based on the solutions of continuous problems.

The optimization procedure was tested with different test cases which included different loads, geometry and steel grades. From the results it was found that there were no difference between mass and cost optimums of the frame. The evaluation of cost components proved that the major part of total costs, almost 80%, was comprised of material costs. This explained why cost optimization returned same solutions as mass optimization.

The quality of optimum solutions was estimated based on the utilization of profiles. The utilization rates remained high in most test cases. In some cases the utilization rates of chords were relatively low due to constraints of welded truss joint resistances.

In such cases evaluation should be made whether a more cost-effective structure is achieved by reinforcing the most heavily loaded joints. The reinforcement of joints should be considered especially in situations where only few joints decide the chord profile.

The use of high-strength steels was studied by comparing the hybrid frame with steel grades S700/S420 and the conventional frame with grades S420/S355. A much lighter structure was achieved in the case of HSS-frame. The total mass of the structure was reduced by more than 10% when grade S700 was exploited for chords. However, the cost difference between frames was virtually non-existent with the material cost factor used in calculations. In practice the price of high-strength steels should be discussed in more detail with the manufacturer so that more accurate costs could be calculated for HSS-frame.

The total calculation time of the four-stage procedure varied between 11 and 19 minutes depending on a size of the FE-model of the frame. It should be also acknowledged that implementation has an influence on the calculation time. The standard deviation of optimum solutions produced by the method was studied with 10 different optimization runs. The results indicated that variability of solutions was very low. The standard deviation was at most 3% in mass and cost optimization. Based on relatively short calculation time and low variability it can be concluded that the method is well suited to a situation in which a good estimate of the optimum profiles and costs are needed to search quickly based on the data including loads and geometry of the frame. Therefore it can be stated that the goal of this thesis was reached.

The available calculation capacity in this study was rather limited which should also be taken into account when assessing the calculation time. Moving calculation from the desktop computer to the separate server could speed up calculation substantially. Consequently, the maximum number of function evaluations in continuous problem and the population size in Genetic Algorithm could be raised. Also parallel calculation could be employed in continuous problem where several starting points are solved. In addition to this, the FE-model of the structure could be built with some commercial design program instead of MATLAB environment.

Further research avenues include improving the discrete problem solution method. Genetic Algorithm could be replaced by some other algorithm that is not population-based. Thus, the optimization time could be reduced even though the time remained moderate with this developed method.

The second research aspect is to expand the size of the optimization problem to

involve serviceability limit state and fire design criteria as well. This study included full inspection of ultimate limit state and geometrical restrictions of joints. By taking into account also serviceability and fire design the optimization problem of the frame would feature all the relevant design criteria.

BIBLIOGRAPHY

[1] J. Arora, "Methods for discrete variable structural optimization," in *Recent Advances in Optimal Structural Design*, S. A. Burns, Ed. ASCE, 2002, pp. 1–40.

[2] J. S. Arora, *Introduction to Optimum Design.* Elsevier Academic Press, 2004.

[3] J. Arora and M.-W. Huang, "Discrete structural optimization with commercially available sections," *Structural Engineering/Earthquake Engineering*, vol. 13, pp. 93–110, 1996.

[4] J. Arora, M.-W. Huang, and G. Hsieh, "Methods for optimization of nonlinear problems with discrete variables: a review," *Structural optimization*, vol. 8, pp. 69–85, 1994.

[5] J. Arora and Q. Wang, "Review of formulations for structural and mechanical system optimization," *Structural and Multidisciplinary Optimization*, vol. 30, pp. 251–272, 2005.

[6] R. Balling, "Optimal steel frame design by simulated annealing," *Journal of Structural Engineering*, vol. 117, pp. 1780–1795, 1991.

[7] B. Davison and G. Owens, *The Steel Designer's Manual.* Wiley-Blackwell, 2011.

[8] EC 3 NA, *National Annex to Standard Eurocode 3: Design of Steel Structures. Part 1-1: General rules and rules for buildings.* Ministry of Environment, Finland, 2005.

[9] EN 1990, *Eurocode: Basis of structural design.* CEN, 2001.

[10] EN 1991–1–1, *Eurocode 1: Actions on structures. Part 1-1: General actions – Densities, self-weight, imposed loads for buildings.* CEN, 2001.

[11] EN 1993–1–1, *Eurocode 3: Design of Steel Structures. Part 1-1: General rules and rules for buildings.* CEN, 2005.

[12] EN 1993–1–8, *Eurocode 3: Design of Steel Structures. Part 1-8: Design of joints.* CEN, 2005.

[13] J. Farkas, L. M. C. Simões, and K. Jármai, "Minimum cost design of a welded stiffened square plate loaded by biaxial compression," *Structural and Multidisciplinary Optimization*, vol. 29, pp. 298–303, 2005.

[14] M. Feldmann, N. Schillo, S. Schaffrath, K. Virdi, T. Björk, N. Tuominen, M. Veljkovic, M. Pavlovic, P. Manoleas, M. Heinisuo, K. Mela, P. Ongelin, I. Valkonen, J. Minkkinen, J. Erkkilä, E. Pétursson, M. Clarin, A. Seyr, L. Horváth, B. Kövesdi, P. Turán, and B. Somodi, "Rules on high strength steel (ruoste)," European Commission, Tech. Rep., 2016.

[15] C. Floudas, *Nonlinear and Mixed-Integer Optimization, Fundamentals and Applications.* Oxford University Press, 1995.

[16] D. Greiner, G. Winter, and J. M. Emperador, "Optimising frame structures by different strategies of genetic algorithms," *Finite Elements in Analysis and Design*, vol. 37, pp. 381–402, 2001.

[17] G. Guerlement, R. Targowski, W. Gutkowski, J. Zawidzka, and J. Zawidzki, "Discrete minimum weight design of steel structures using ec3 code," *Structural and Multidisciplinary Optimization*, vol. 22, pp. 322–327, 2001.

[18] J. Haapio, "Feature-based costing method for skeletal steel structures based on the process approach," Ph.D. dissertation, Tampere University of Technology, 2012.

[19] R. T. Haftka and Z. Gurdal, *Elements of Structural Optimization.* Kluwer Academic Publishers, 1992.

[20] K. Hager and R. Balling, "New approach for discrete structural optimization," *Journal of Structural Engineering*, vol. 114, pp. 1120–1134, 1988.

[21] J. Holland, *Adaptation in natural and artificial systems.* Ann Arbor: University of Michigan Press, 1975.

[22] J. Jalkanen, "Tubular truss optimization using heuristic algorithms," Ph.D. dissertation, Tampere University of Technology, 2007.

[23] K. Jármai and J. Farkas, "Optimum cost design of welded box beams with longitudinal stiffeners using advanced backtrack method," *Structural and Multidisciplinary Optimization*, vol. 21, pp. 52–59, 2001.

[24] K. Jármai and J. Farkas, "Cost calculation and optimisation of welded steel structures," *Journal of Constructional Steel Research*, vol. 50, pp. 115–135, 1999.

[25] G. Nemhauser and L. Wolsey, *Integer and Combinatorial Optimization.* John Wiley & Sons, 1999.

[26] P. Ongelin and I. Valkonen, *SSAB Domex Tube, Structural hollow sections, EN 1993 - handbook*. SSAB Europe Oy, 2016.

[27] J. A. Packer, J. Wardenier, X.-L. Zhao, A. van der Vegte, and Y. Kurobane, *Design Guide for Rectangular Hollow Section (RHS) Joints Under Predominantly Static Loading*, 2nd ed. CIDECT, 2009.

[28] L. Pavlovčič, A. Krajnc, and D. Beg, "Cost function analysis in the structural optimization of steel frames," *Structural and Multidisciplinary Optimization*, vol. 28, pp. 286–295, 2004.

[29] R. Stroetmann, "High strength steel for improvement of sustainability. proceedings of the eurosteel 2011 conference," Budapest, Hungary, Sep. 2011.

[30] P. Thanedar and G. Vanderplaats, "Survey of discrete variable optimization for structural design," *Journal of Structural Engineering*, vol. 121, pp. 301–306, 1995.

[31] T. Tiainen and K. Mela, "Kaksivaiheinen menettely epälineaarisen diskreetin teräsrakenteiden optimointitehtävän ratkaisemiseksi," *Rakenteiden Mekaniikka*, vol. 50, pp. 118–121, 2017.

[32] Q. Wang and J. S. Arora, "Alternative formulations for structural optimization: An evaluation using frames," *Journal of Structural Engineering*, vol. 132, no. 12, pp. 1880–1889, 2006.

APPENDIX A. SHS PROFILE CATALOG

The SHS profiles that are used for the discrete optimization problem are presented in Table A.1. The profiles are chosen from SSAB Domex Tube (S355 and S420) and Strenx Tube -catalog (S700). Only Cross-section classes 1 and 2 are included. In the table, h is the side length and t is the wall thickness of the profile. The steel grades available for the profile are also indicated in the table.

Table A.1: *SHS-profiles.*

h [mm]	t [mm]	Steel grade [-]	h [mm]	t [mm]	Steel grade [-]
50	3	S355, S420	150	6	S355, S420, S700
50	4	S355, S420	150	7.1	S355, S420
50	5	S355, S420	150	8	S355, S420, S700
60	3	S355, S420	150	8.8	S355, S420
60	4	S355, S420	150	10	S355, S420, S700
60	5	S355, S420	150	12.5	S355, S420
70	3	S355, S420	160	5	S355
70	4	S355, S420	160	6	S355, S420
70	5	S355, S420	160	7.1	S355, S420
80	3	S355, S420	160	8	S355, S420, S700
80	4	S355, S420, S700	160	8.8	S355, S420
80	5	S355, S420, S700	160	10	S355, S420, S700
80	6	S355, S420, S700	160	12.5	S355, S420
90	3	S355, S420	180	6	S355, S420
90	4	S355, S420, S700	180	7.1	S355, S420
90	5	S355, S420, S700	180	8	S355, S420, S700
90	6	S355, S420	180	8.8	S355, S420
100	3	S355	180	10	S355, S420, S700
100	4	S355, S420, S700	180	12.5	S355, S420
100	5	S355, S420, S700	200	6	S355
100	6	S355, S420, S700	200	7.1	S355, S420
100	7.1	S355, S420	200	8	S355, S420, S700
100	8	S355, S420, S700	200	8.8	S355, S420
100	10	S355, S420	200	10	S355, S420, S700
110	4	S355, S420	200	12.5	S355, S420
110	5	S355, S420	220	7.1	S355, S420
110	6	S355, S420	220	8	S355, S420
120	4	S355, S420	220	8.8	S355, S420
120	5	S355, S420, S700	220	10	S355, S420, S700
120	5.6	S355, S420	220	12.5	S355, S420
120	6	S355, S420, S700	250	7.1	S355
120	7.1	S355, S420	250	8	S355, S420
120	8	S355, S420, S700	250	8.8	S355, S420
120	8.8	S355, S420	250	10	S355, S420, S700
120	10	S355, S420	250	12.5	S355, S420
140	5	S355, S420	260	8	S355
140	5.6	S355, S420	260	8.8	S355, S420
140	6	S355, S420, S700	260	10	S355, S420
140	7.1	S355, S420	260	12.5	S355, S420
140	8	S355, S420, S700	300	8.8	S355
140	8.8	S355, S420	300	10	S355, S420
140	10	S355, S420, S700	300	12.5	S355, S420
150	5	S355, S420			